https://doi.org/10.5194/bg-2021-82
Preprint. Discussion started: 6 April 2021

Biogeosciences Discussions

Particulate organic carbon budget of the Gulf of Lion shelf (NW Mediterranean) using a coupled hydrodynamic-biogeochemical model

Many Gaël[1], Ulses Caroline[1,2], Estournel Claude[1,2], Marsaleix Patrick[2]
1 Laboratoire d'Aérologie, Université de Toulouse, CNRS, UPS, 14 Avenue Edouard Belin, 31400 Toulouse, France
2 LEGOS, Université de Toulouse, CNES, CNRS, IRD, UPS, 14 Avenue Edouard Belin, 31400 Toulouse, France
Correspondence to: Gaël Many (gael.many@outlook.fr)

Abstract. The Gulf of Lion shelf (NW Mediterranean) is one of the most productive areas in the Mediterranean Sea. A 3D coupled hydrodynamic-biogeochemical model is used to study the mechanisms that drive the particulate organic carbon (POC) budget over the shelf. A set of observations, including temporal series from a coastal station, remote sensing of surface chlorophyll-a, and a glider deployment, is used to validate the distribution of physical and biogeochemical variables from the model. The model reproduces well the time and spatial evolution of temperature, chlorophyll, and nitrate concentrations and shows a clear annual cycle of gross primary production and respiration. Knowing the physical and biogeochemical inputs and outputs terms, the annual budget of the POC in the Gulf of Lion is estimated and discussed. We estimate an annual net primary production of ~200 10^4 tC yr^{-1} at the scale of the shelf. The primary production is marked by a coast-slope increase with maximal values in the eastern region. Our results show that the primary production is favored by the inputs of nutrients imported from offshore waters, representing 3 and 15 times the inputs of the Rhône in terms of nitrate and phosphate. Besides, the EOFs decomposition highlights the role of solar radiation anomalies and continental winds that favor upwellings, and inputs of the Rhône River, on annual changes in the net primary production. Annual POC deposition (19 10^4 tC yr^{-1}) represents 10% of the net primary production. The delivery of terrestrial POC favored the deposition in front of the Rhône mouth and the mean cyclonic circulation increases the deposition between 30 and 50 m depth from the Rhône prodelta to the west. Mechanisms responsible for POC export (24 10^4 tC yr^{-1}) to the open sea are discussed. The export off the shelf in the western part, from the Cap de Creus to the Lacaze-Duthiers canyon, represented 37% of the total POC export. Maximum values were obtained during shelf dense water cascading events and marine winds. Considering surface waters only, the POC was mainly exported in the eastern part of the shelf through shelf waters and Rhône inputs, which spread to the Northern Current during favorable continental wind conditions. The Gulf of Lion shelf appears as an autotrophic ecosystem with a positive Net Ecosystem Production and as a source of POC for the adjacent NW Mediterranean basin. The undergoing and future increase in temperature and stratification induced by climate change could impact the trophic status of the GoL shelf and the carbon export towards the deep basin. It is crucial to develop models to predict and assess these future evolutions.

https://doi.org/10.5194/bg-2021-82
Preprint. Discussion started: 6 April 2021

1. Introduction

1.1 The importance of continental margins in the organic carbon budget

Continental margins are of particular interest concerning the input, production, deposition, and export to the deep open ocean of particulate organic carbon (POC) (Bauer and Druffel, 1998; Liu et al., 2010). These buffer regions often show high biological productivity, induced by solar radiation and nutrients availability from river inputs and coastal upwellings (Legendre, 1990; Dagg et al., 2004; Lohrenz et al., 2008). The input of terrigenous POC and this high productivity make these coastal zones areas of high organic matter deposition (Gao and Wang, 2008; Dagg et al., 2008). Hydrodynamic processes such as upwelling, dense water cascading, slope current could favor the lateral transport of POC towards the open sea and deeper environments (Lapouyade and Durrieu de Madron, 2001; Thunell et al., 2007; Sanchez-Vidal et al., 2008). The understanding of the input, deposition, and export of POC is thus essential to estimate the carbon budgets of coastal areas at a world scale.

Besides, modeling the POC dynamics in coastal and shelf systems needs the integration of several processes interacting with each other, as a land-sea continuum (riverine organic carbon and nutrient inputs) and hydrodynamical forcings on POC production and transport in the water column. A realistic simulation of the hydrodynamical processes in the coastal area is essential to reproduce the spatiotemporal changes in POC conditions (Hofmann et al., 2011). Among those processes, circulation patterns and stratification dynamics are considered to be extremely important to describe the POC horizontal advection, impacted by water mass upwelling, and shelf-open ocean water mass exchanges, as well as to be able to describe the vertical gradients in nutrient conditions that control the POC production (primary production) and the POC deposition (Liu and Chaï, 2009).

1.2 Regional settings

The Gulf of Lion shelf (GoL) in the NW Mediterranean is a wide continental shelf (Fig. 1, area of approximately 10 000 km²) strongly influenced by freshwater and particulate matter inputs from the Rhône River (Fig. 1). The Rhône River is characterized by a mean annual discharge of 1,700 $m^3 s^{-1}$, which makes the GoL one of the most river-impacted areas of the Mediterranean (Naudin et al., 1997; Maillet et al., 2006; Ludwig et al., 2009). Sadaoui et al. (2016) estimated a total suspended solid flux around 8.4 10^6 t yr^{-1} from which approximately 1% is considered as POC (see Table 2 in Durrieu de Madron et al., 2000). During floods, terrestrial inputs from the Rhône create a surface plume that spreads southward across the shelf by surface currents driven by continental (westerly/northerly) winds or is constrained along the coast during marine (easterly) winds. Besides, Rhône inputs also feed a bottom nepheloid layer that favors local sediment deposition (Many et al., 2018). The Gulf of Lion is bordered on the continental slope by the Northern Current associated with the general circulation of the western Mediterranean basin (Petrenko et al., 2008).

https://doi.org/10.5194/bg-2021-82
Preprint. Discussion started: 6 April 2021

In terms of biological net primary production (NPP), the Gulf of Lion is one of the most productive areas in the Mediterranean Sea (together with the North Adriatic and the Alboran Sea) (Bosc et al., 2004). It is an exception in this oligotrophic system, which is relatively impoverished in nutrients concerning the open ocean. The annual production in the GoL shelf has been estimated to be in the range of 80-150 gC m^{-2} yr^{-1} (90-165 10^4 tC yr^{-1} considering a shelf area of 1.1 10^{10} m^2) (Durrieu de Madron et al., 2000), which is similar to the production in the adjacent deep-water formation area (Lefevre et al., 1997; Ulses et al., 2016; Kessouri et al., 2018).

The main mechanisms that drive POC deposition in the Gulf of Lion are widely described in Auger et al. (2011). The authors highlighted the contribution of organic detritus to 80-90% of the total POC deposition whereas the contribution of living particles (phytoplankton) was estimated to approx. 10-20%. Besides, the authors estimated that the contribution of terrestrial particulate organic carbon corresponds to less than 17 % of the total of POC deposition, with the main deposition occurring in front of the Rhône mouth during floods. On the other hand, the predominant influence of marine biological production on POC deposition over the entire shelf is highlighted.

The Gulf of Lion is considered as a source of POC to the basin of the NW Mediterranean sea (Durrieu de Madron et al., 2000; Ulses et al., 2008b; Ulses et al., 2016). It is a very dynamic system, marked by low residence times (Mikolajczak et al., 2020) where wind-induced currents are important for POC horizontal advection. Coastal hydrodynamic conditions are influenced by the circulation along the continental slope, the Northern Current (Petrenko et al., 2003), the freshwater inputs from the Rhône (Marsaleix et al., 1998; Estournel et al., 2001), the wind-driven circulation over the shelf (Estournel et al., 2003; Petrenko, 2003; Petrenko et al., 2005; Ulses et al., 2008a), and the formation and cascading of shelf dense water (Dufau-Julliand et al., 2004; Ulses et al., 2008c).

It is however noticeable that the values of the POC budget terms have been determined based on local observations and/or during limited periods. The inter-annual variability of the environmental conditions (wind velocity, heat flux, temperature, etc.) as well as episodic events (floods, storms, water mass upwellings) are also expected to play a key role in changes in the POC budget over the shelf and need to be quantified.

1.3 Objective of this study

The objective of this present work is to estimate the POC budget on the Gulf of Lion shelf and to improve our understanding of the mechanisms that control this budget based on a coupled hydrodynamical-biogeochemical model over a pluriannual period. The 2011-2016 period was characterized by high annual changes in environmental conditions, particularly during winters, which are key periods in the water mass export and mixing, and phytoplankton bloom triggering (see winter heat fluxes and winds in Fig. 1). The 2011-2012 and 2014-2015 periods were marked by cold winters with strong heat losses. The 2013-2014 and 2015-2016 periods were characterized by mild winters. The Rhône River discharge was minimal in 2011-2012 and maximal in 2012-2013. At last, winter 2015-2016 was a period characterized by severe marine storms (see the wind rose

https://doi.org/10.5194/bg-2021-82
Preprint. Discussion started: 6 April 2021

95 in Fig. 1). It is expected that these variations in these environmental conditions, that may influence the availability of nutrients in the surface layer, and hence the phytoplankton growth will affect the POC budget on the shelf, which remains seldom quantified at the scale of the shelf and during contrasted years.

In this paper, we present the numerical model used to carry out this study, particularly its validation against multiplatform
100 observations including time series from a coastal station, remote sensing of surface chlorophyll-a, and a glider deployment to describe the vertical distributions of physical and biogeochemical conditions. After describing the environmental conditions, we then estimate the POC budget of the shelf during the 2011-2016 period, and detail and discuss the variability of the nutrient availability, primary production, the deposition over the shelf, and the cross-shelf transport of POC towards the deep basin and the Catalan margin over this period marked by contrasted meteorological, hydrodynamic and fluvial conditions.

https://doi.org/10.5194/bg-2021-82
Preprint. Discussion started: 6 April 2021

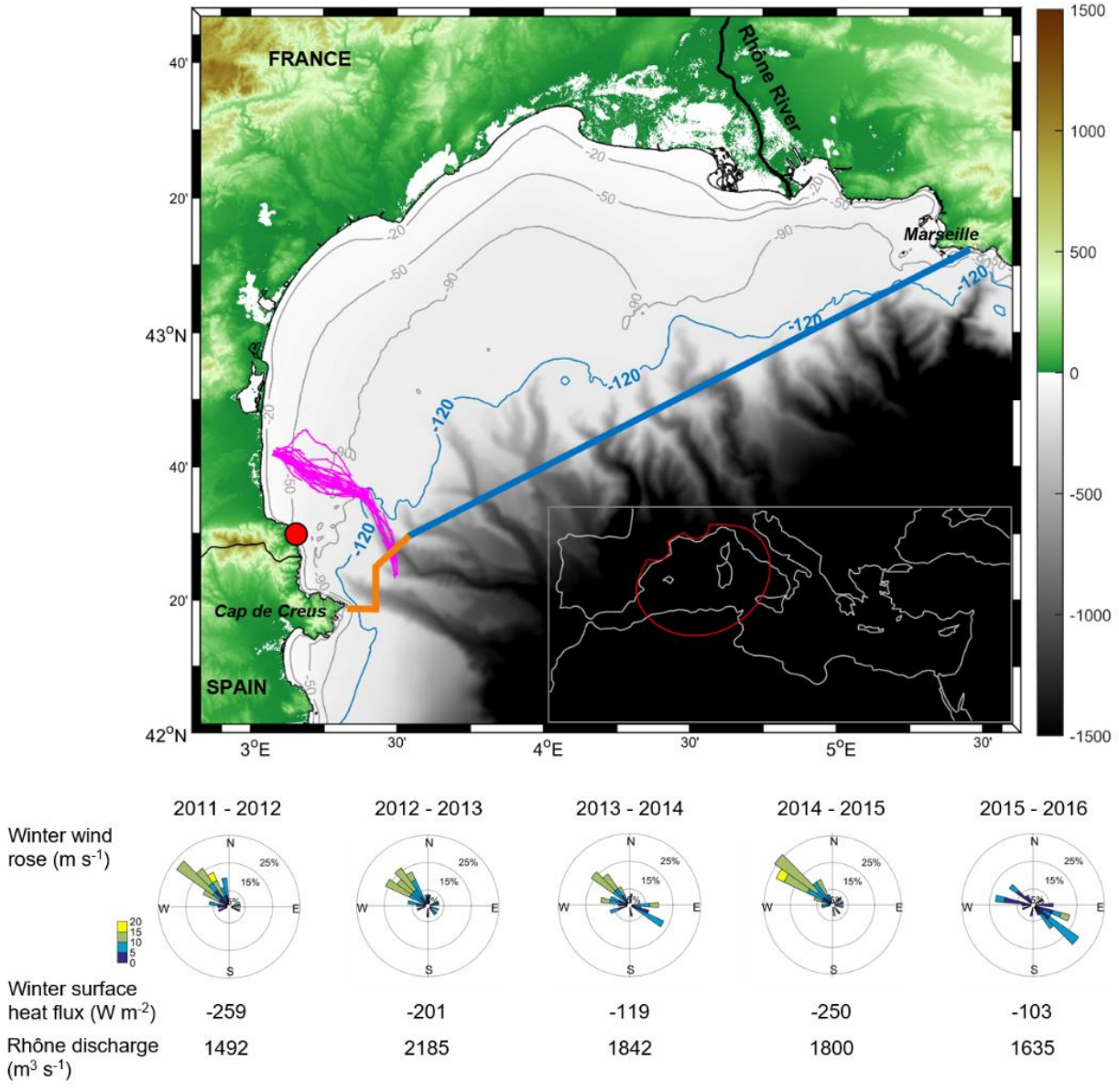

105

Figure 1: Top: Bathymetry (m) of the Gulf of Lion (NW Mediterranean Sea). The Rhône River is shown by a black line. SOMLIT Banyuls station is shown in red. The path of the glider during the April/May 2013 deployment is shown in magenta. The limit of the shelf studied in this work is specified by the 120 m isobath. The thick blue and orange lines show the limit of the boundaries used to estimate water, nutrients, and particulate organic carbon transports in the eastern and western part of the shelf, respectively. The 110 **boundary of the model grid is shown in red on the inserted Mediterranean map. Bottom: Meteorological and fluvial forcings for each year simulated: the winter (DJF) mean wind rose (m s^{-1}), winter surface heat flux (W m^{-2}), and annual Rhône River discharge (m^3 s^{-1}) are specified.**

https://doi.org/10.5194/bg-2021-82
Preprint. Discussion started: 6 April 2021

2. Material and methods

2.1 The model

The three-dimensional model results from the off-line forcing of the biogeochemical Eco3M-S model by the regional circulation SYMPHONIE model. These two models and the coupling procedure are described thereafter.

2.1.1 The hydrodynamic model

The SYMPHONIE model (Marsaleix et al., 2006; 2008) is a 3-D primitive equation, free surface, and generalized sigma vertical coordinate model. This model was previously used to simulate the hydrodynamic conditions in the Mediterranean Sea and specific processes as the Rhone river plume dynamics (Estournel et al., 1997; Reffray et al, 2004), coastal dense water formation (Ulses et al., 2008c), wind-induced circulation over the Gulf of Lion shelf (Estournel et al., 2003; Petrenko et al., 2008; Ulses et al., 2008a), shelf-slope exchanges and along-slope circulation (Bouffard et al., 2008; Mikolajczak et al., 2020).

The numerical grid of the model is the same as in the study of Briton et al. (2018). It consists of a curvilinear bipolar (Bentsen et al, 1999) Arakawa C-grid with 40 vertical sigma levels (Mikolajczak et al., 2020). The bipolar grid presents a horizontal resolution between 300 m and 500 m over the shelf, and gradually decreases to several km towards the south of the domain along the Algerian coast. This configuration allows us to have more than half of the total points of the grid over the shelf while keeping the open boundaries far from the study area, the Gulf of Lion.

River runoffs were considered using measured daily values for French rivers (Banque Hydro database, www.hydro.eaufrance.fr), the Ebro (SAIH Ebro database, www.saihebro.com), and mean annual value for the others. The implementation of rivers in the model was described in Estournel et al. (2009). Atmospheric forcings were generated by the hourly fields (wind speed and direction, pressure, air temperature and humidity, solar and downward longwave radiation and precipitation) provided by the ECMWF (European Centre for Medium-Range Weather Forecasts) forecasts. We used the bulk formula of Large and Yeager (2004) to estimate the surface turbulent fluxes.

The period simulated with the SYMPHONIE model runs from 1 July 2011 to 31 December 2016. The initial state and the open boundary conditions were generated by a "parent" simulation (SYMPHONIE) that began two months earlier than the "child" simulation. The open lateral boundary conditions of the child model consist of radiative conditions reinforced by a lateral restoring layer towards the hydrodynamic fields of the parent model (Marsaleix et al, 2006). The parent model covers the Mediterranean basin. Its average horizontal resolution is 4 km. It is initialized with the Mercator Ocean International operational center hydrodynamic fields using the stratification index correction method described in Estournel et al. (2016).

2.1.2 The biogeochemical model

The Eco3M-S model is a multi-plankton and multi-nutrient dynamics model (Ulses et al., 2016) that simulates the dynamics of the biogeochemical cycles of biogenic elements (carbon, nitrogen, phosphorus, silicon, and oxygen) and plankton groups.

https://doi.org/10.5194/bg-2021-82
Preprint. Discussion started: 6 April 2021

The model structure with seven compartments (see Fig. 2 in Kessouri et al. 2017) is described in Auger et al. (2011), Ulses et al. (2016), and Kessouri et al. (2017).

We used the "Source Splitting" coupling method (Butenschön et al., 2012), which consists of an off-line forcing of the biogeochemical model by the daily averaged outputs of the physical model. It is then assumed that biogeochemical properties do not significantly impact hydrodynamics and we used a time step of 10 minutes for the advection and diffusion of biogeochemical variables.

Rhône River nutrient inputs (nitrate, ammonium, phosphate, silicate, and dissolved organic carbon) were determined using *in situ* daily data (Mistrals-Sedoo database, http://mistrals.sedoo.fr/MOOSE/). Concentrations of dissolved organic phosphorus and nitrogen and particulate organic carbon were estimated from this dataset and the relations found in the literature (Moutin et al., 1998; Sempéré et al., 2000). The Orb, Aude, and Herault rivers monthly data were extracted from the Naïades database (Agence de l'eau, http://www.naiades.eaufrance.fr/) and were interpolated on the period of the simulation with a daily resolution. At the other river (Tech, Têt, Agly) mouths, climatological values were used according to Ludwig et al. (2010). The deposition of organic and inorganic matter from the atmosphere was based on the low estimations of Ribera d'Alcala et al. (2003). Finally, the pelagic-benthic coupling of inorganic nutrients was made using the meta-model described in Soetaert et al. (2001). An adjustment of this model was made according to Pastor et al. (2011).

As for the hydrodynamic model, the initial state and the open boundary conditions were generated by a "parent" simulation (Eco3M-S) that encompassed the whole Mediterranean Sea. This latter simulation was forced by the same daily fields from the SYMPHONIE model as used for the "child" regional hydrodynamic model (see 2.1.1). This ensures the coherence of the physical and biogeochemical fields at the open boundaries of the child regional model. The period simulated with the Eco3M-S regional model runs from 1 August 2011 to 31 July 2016.

2.2 Observations used for the model evaluation

2.2.1 SOMLIT data

Long-term measurements from the Banyuls (42.492°N; 3.153°E) SOMLIT (Service d'Observation en Milieu Littoral) station were downloaded from the SOMLIT website (http://somlit-db.epoc.u-bordeaux1.fr/bdd.php). Daily time series of temperature, salinity, nutrients (nitrate, phosphate), particulate organic carbon were extracted at the surface (~2 m depth) and close to the bottom (~2 m above the bottom, i.e. ~25 m depth). The description of the data acquisition is detailed in Fraysse et al. (2013) and Liénart et al. (2017; 2018).

2.2.2 Satellite data

Spatial maps of daily chlorophyll-a concentrations, with a 1 km resolution, were obtained using products from Moderate Resolution Imaging Spectroradiometer (MODIS). Products, analysis, and calibrations used were provided by IFREMER

https://doi.org/10.5194/bg-2021-82
Preprint. Discussion started: 6 April 2021

Nausicaa services and OC5 IFREMER algorithms for Chl-a concentrations from Gohin (2011). We then estimated the daily spatial median surface chlorophyll-a concentration (in µg L^{-1}) using a filter to discard images with more than 50% occupied by clouds over the GoL and discarding surface chlorophyll-a data for depth lower than 20 m since these data could be affected by residual contamination from turbidity despite dedicated treatment.

2.2.3 Glider-based measurements

The glider-based time series (Testor et al., 2018) consist of lines of 25 to 50 km long that run across the shelf from the coast (30 m depth) to the shelf edge (100 m water depth) in the vicinity of the Lacaze-Duthiers canyon head (SW Gulf of Lion) (see glider path in Fig. 1). The autonomous glider was a coastal Teledyne Webb Research Slocum (Davis et al., 2002) that moved at an average speed of 20–30 cm s^{-1} in a sawtooth-shaped trajectory between 1 m below the surface and 1–2 m above the seabed. The glider was equipped with an un-pumped Seabird 41-CP CTD providing temperature, depth, and conductivity data. Salinity was derived following the equation of EOS-80. We then derived the Brunt-Väisälä frequency (N^2 expressed in s^{-2}), which was used as an indicator of the thermal stratification (see details in Many et al. (2018)).

A Wetlabs FLNTU sensor provided turbidity (expressed in NTU) and fluorescence of chlorophyll-a (factory calibrated and expressed in µg L^{-1}) measurements based on backscattering measurements at 700 nm. Turbidity measurements from the FLNTU (λ = 700 nm) optical sensor of the glider were used to estimate the particulate backscattering coefficients bbp_{700}, which were used to correct fluorescence data from the nonphotochemical quenching (NPQ) (Sackmann et al., 2008; Behrenfeld et al., 2009). The correction applied was determined using the night and day bbp_{700} and fluorescence profiles (see details in Thomalla et al. (2018)).

3. Model evaluation

3.1 Observations/model comparisons at the Banyuls SOMLIT station

Comparisons of simulated surface and bottom temperature and salinity with those measured at the Banyuls SOMLIT station for the period 2011-2016 are presented in Fig. 2. The highly significant correlation (i.e. coefficient of determination $R^2>0.8$ for surface data and $R^2>0.6$ for bottom data, $p<0.01$), the RMSD inferior to 0.6, and normalized standard deviation of approx. 1 at the surface suggest that the model reproduces the main changes in physical conditions induced by the variability of heat and water flux and the impact of freshwater discharge.

https://doi.org/10.5194/bg-2021-82
Preprint. Discussion started: 6 April 2021

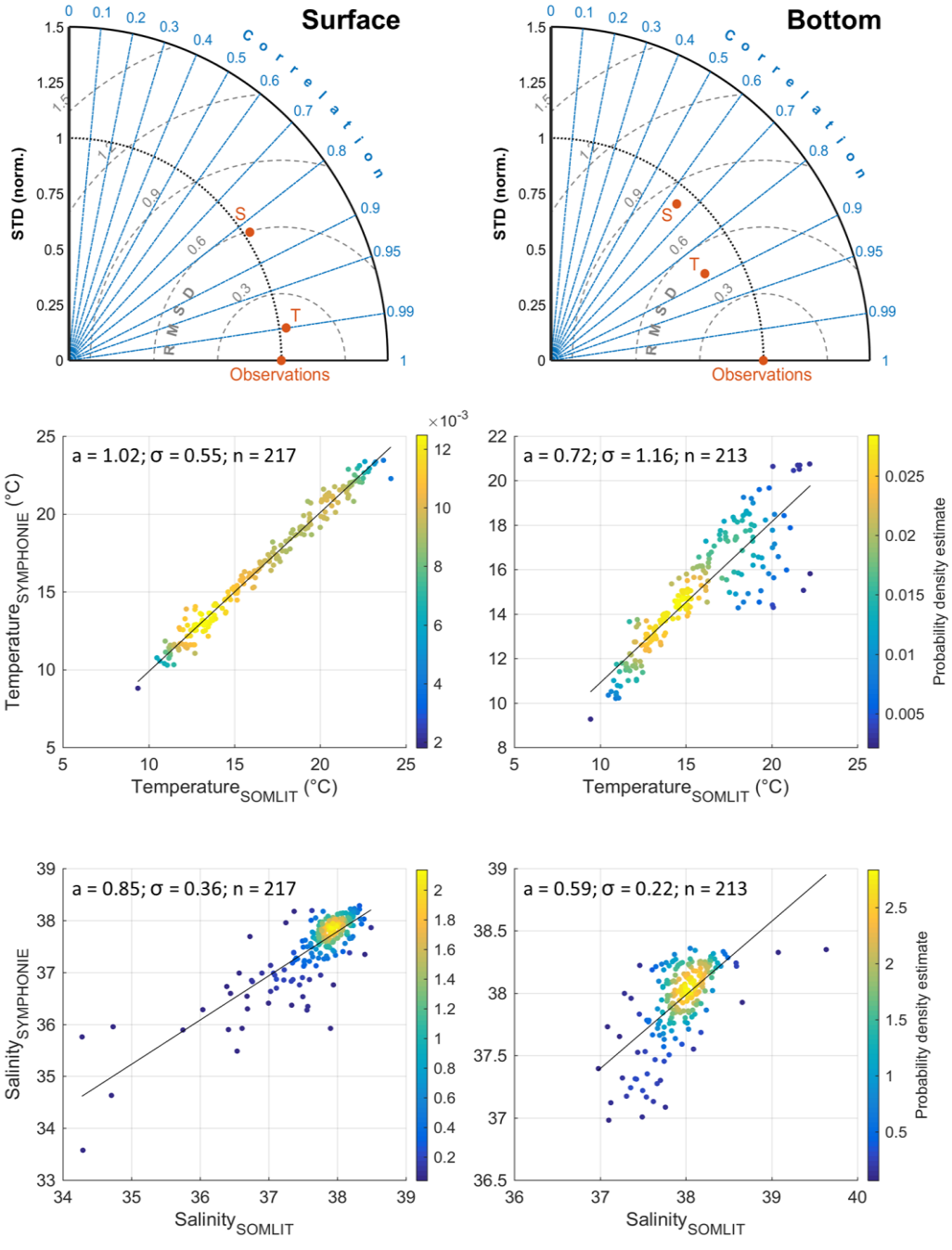

200 **Figure 2: Comparison of simulated and measured (SOMLIT) temperature (T in top panels) (°C) and salinity (S in top panels) at the surface (left) and bottom (right) layers for the period 2011-2016. The scatter plots show the density of points (i.e. the kernel density estimation of simulation-observation pairs). The slope of the relation (a), the standard deviation (σ), and the number of data (n) are specified.**

https://doi.org/10.5194/bg-2021-82
Preprint. Discussion started: 6 April 2021

At the SOMLIT coastal station, the model captures the annual cycle in Chl-a, NO_3, PO_4, and POC concentrations for surface and bottom waters (Fig. 3). If the model estimates well Chl-a concentrations in summer, the maximum concentrations in winter/spring are systematically underestimated in the model. The underestimation is more pronounced at the surface than near the bottom. The temporal evolution and magnitude of the modeled nitrate are close to that observed, while the modeled PO_4 concentrations were significantly lower in the model than in the observations, in particular near the surface. The discrepancy in PO_4 concentration could be explained by the too rapid consumption of this nutrient by phytoplankton in the model. POC concentrations were well estimated in the model (slope of approx. 0.9), which allow the exploitation of the results as part of the POC budget estimate.

https://doi.org/10.5194/bg-2021-82
Preprint. Discussion started: 6 April 2021

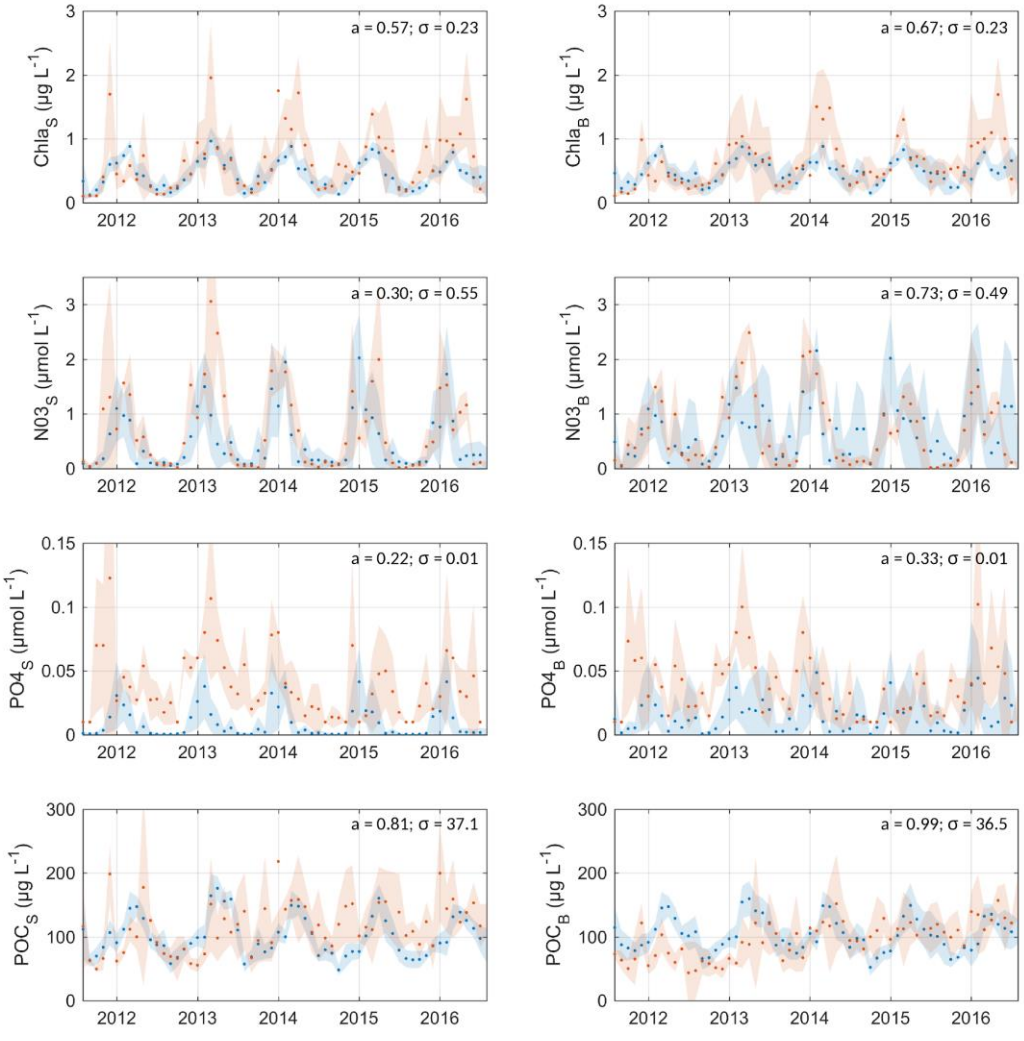

Figure 3: Comparison of monthly averaged simulated (blue) and measured (orange - SOMLIT Banyuls station) concentration of (from top to bottom) Chl-a (µgChl L^{-1}), NO_3 (µmolN L^{-1}), PO_4 (µmolP L^{-1}), and POC (µgC L^{-1}) from the surface (left) and bottom (right) waters. Standard deviations are shown by shaded areas. The slope of the linear relation model to observation (a) and the mean standard deviation (σ) are specified. Note that here the bacteria and mesozooplankton concentrations are excluded from the POC calculation to fit with the measurement method.

3.2 Surface Chlorophyll-a comparison between MODIS and model for the period 2011-2016

The comparison of the daily mean value of the surface chlorophyll-a, measured from MODIS and extracted from the model at the same points and days, averaged over the GoL shelf is shown in Fig. 4. We obtain mean chlorophyll-a concentrations from

https://doi.org/10.5194/bg-2021-82
Preprint. Discussion started: 6 April 2021

MODIS and the simulation of 0.39 (±0.23) and 0.35 (±0.24) µg L^{-1} over the 2011-2016 period. The relationship between the binned data shows a very good agreement between the model and the observations (slope=0.8; R^2=0.97; p<0.01) with a mean bias of 0.04 µg L^{-1}. The model reproduces well the seasonality of the surface chlorophyll-a with the main maximum during the spring period (approx. 1 µg L^{-1} at the end of March) and a secondary maximum in fall (approx. 0.6 µg L^{-1}). The spatial patterns with high concentrations in the river plumes were also correctly reproduced (see the bottom panel in Fig. 4). Some discrepancies, however, exist, in particular during spring, where the model could overestimate the surface chlorophyll-a concentrations.

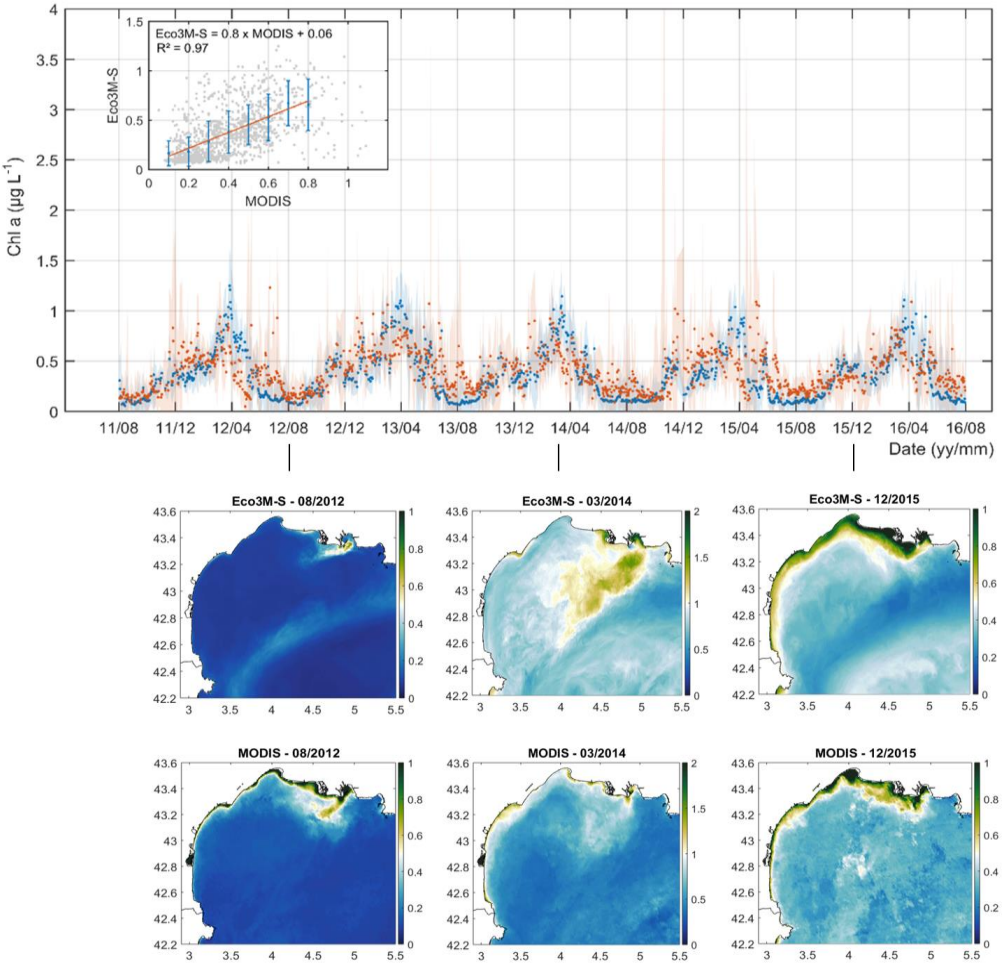

Figure 4: Top: Comparison of the daily mean value of surface chlorophyll-a (µg L^{-1}) from MODIS (orange) and extracted from the Eco3M-S model (blue). The linear relationship is shown in the top-left corner. Standard deviations of each estimate are shown by shaded areas. Bottom: Comparisons of monthly mean surface chlorophyll-a (in µg L^{-1}) from Eco3M-S (top) and MODIS (bottom) in summer 2012, spring 2014, and winter 2015.

https://doi.org/10.5194/bg-2021-82
Preprint. Discussion started: 6 April 2021

3.3 Glider/Model comparison

The comparison between the data from the glider deployment in April/May 2013 and those extracted from the model at the same time and position is shown in Fig. 5. Overall, the comparison shows a good agreement between the descriptions of temperature, salinity, and chlorophyll-a conditions in the model and glider data, with mean biases of 0.33 °C, 0.17, and 0.001 µg L^{-1} respectively. This period was characterized by the establishment of the water column stratification. Temperature, salinity, and Brunt-Väisälä frequency derived from the glider data reflect the vertical stratification that controlled the chlorophyll-a vertical distribution. The model accurately reproduces these vertical thermal and chlorophyll-a distributions, although some differences exist, such as the intensity of the stratification (see the Brunt-Väisälä frequency in Fig. 5)

Chlorophyll-a measurements along the glider path in April/May 2013 indicate frequent occurrences of subsurface chlorophyll-a maxima (approx. 1.5 µg L^{-1}) that is well represented in the model data despite an underestimation of the intensity (see bottom panel on Fig. 5).

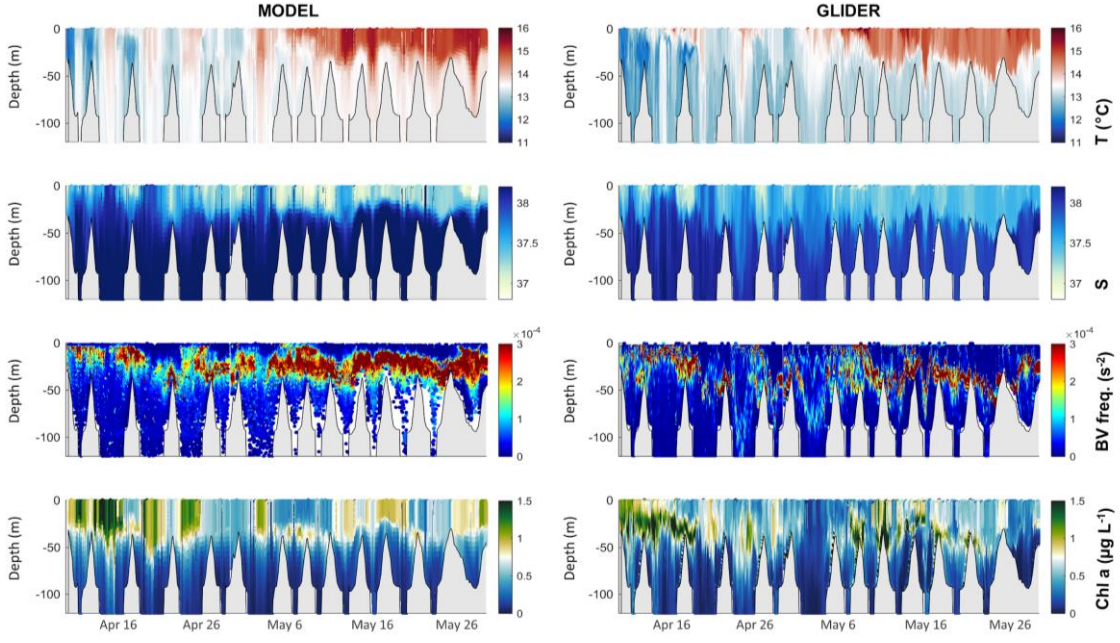

Figure 5: Comparisons of model outputs (left) and glider-based measurements (right) of (from top to bottom): temperature (°C), salinity, derived Brunt-Väisälä frequency (s^{-2}), and chlorophyll-a (µg L^{-1}, corrected from quenching for glider data). Simulated data correspond to the extracted data at the glider time and position. Bathymetry is shown in gray.

https://doi.org/10.5194/bg-2021-82
Preprint. Discussion started: 6 April 2021

4. Results

4.1 Annual cycles and estimates of physical and biogeochemical conditions

4.1.1 Atmospheric, hydrodynamic and fluvial conditions

Time series of the simulated surface solar radiation, heat flux, and stratification index are shown in Fig. 6 (spatially averaged over the GoL shelf). Figure 6b shows that the shelf of the Gulf of Lion lost heat at the air-sea interface from October to mid-March and gained heat from the atmosphere from mid-March to September. Heat flux shows a strong interannual variation between the end of November and mid-February when strong heat loss events occurred, reaching a monthly average of 400 W m^{-2} in February 2012. The stratification of the water column also exhibited a clear annual cycle (Fig. 6c). From October to early December the cold northerly wind events induced a progressive decrease in the stratification. It increased from March until July when the shelf warmed up. The interannual variability appeared quite strong in summer and fall.

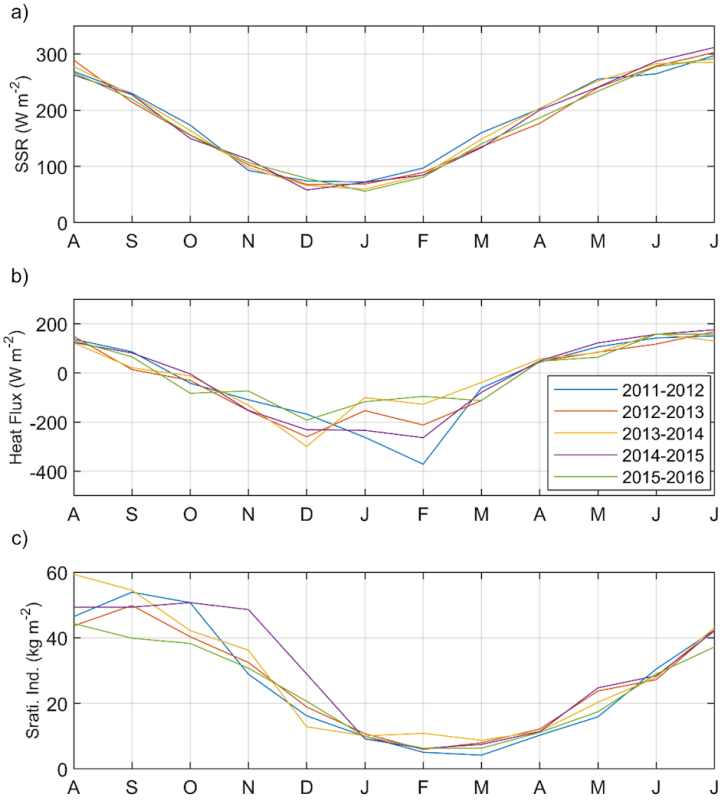

Figure 6: Time series for the five simulated years of monthly a) surface solar radiation (W m^{-2}), b) heat flux (W m^{-2}), c) stratification index (kg m^{-2}).

https://doi.org/10.5194/bg-2021-82
Preprint. Discussion started: 6 April 2021

Volume transport is assessed in Fig. 7 through two unequal sections that close off the Gulf of Lion shelf (see Fig. 1). Besides, the water column is each time divided into two parts, above (Fig. 7a) and below (Fig. 7b) 60 m corresponding roughly to the depth of the nutricline in summer (Kessouri et al., 2017). The "western" section corresponds to the area known to be responsible for deep export by cascading (sometimes down to the bottom of the basin ~2500 m) during cold winters (Ulses et al., 2008c; Durrieu de Madron et al., 2013). This export is restricted to 300-400 m during mild winters and also during eastern storms, which blow predominantly in autumn and produce a downwelling in the Cap de Creus Canyon (Ulses et al., 2008a; Mikolajczak et al., 2020). The other section hereafter named “eastern” for the sake of simplicity is known in the eastern part as an intrusion zone of the Northern Current (Conan et al., 1998), while in the center of the shelf, exchanges with the Northern Current have also been (more rarely) documented (Estournel et al., 2003). It is also the area where the Rhone plume most often exits the shelf under prevailing NW to N wind conditions (Gangloff et al., 2017; Many et al., 2018).

From the end of spring to summer (May-September), the exchanges between the coast and the open sea resulted in an import to the west and export to the east limited to the surface layer and of the order of 0.1 Sv on average (Fig. 7a). In fall (usually October and/or November, brown shaded area on Fig. 7), the shelf imported waters from the east and exported to the west, with exchanges on both layers between 0.1 - 0.2 Sv. In late winter and early spring (roughly from February to April, but especially in 2012 and 2013) the exchanges were in the same direction but took place mostly in the deep layer, reaching 0.2 Sv in February 2012 (Fig. 7b).

https://doi.org/10.5194/bg-2021-82
Preprint. Discussion started: 6 April 2021

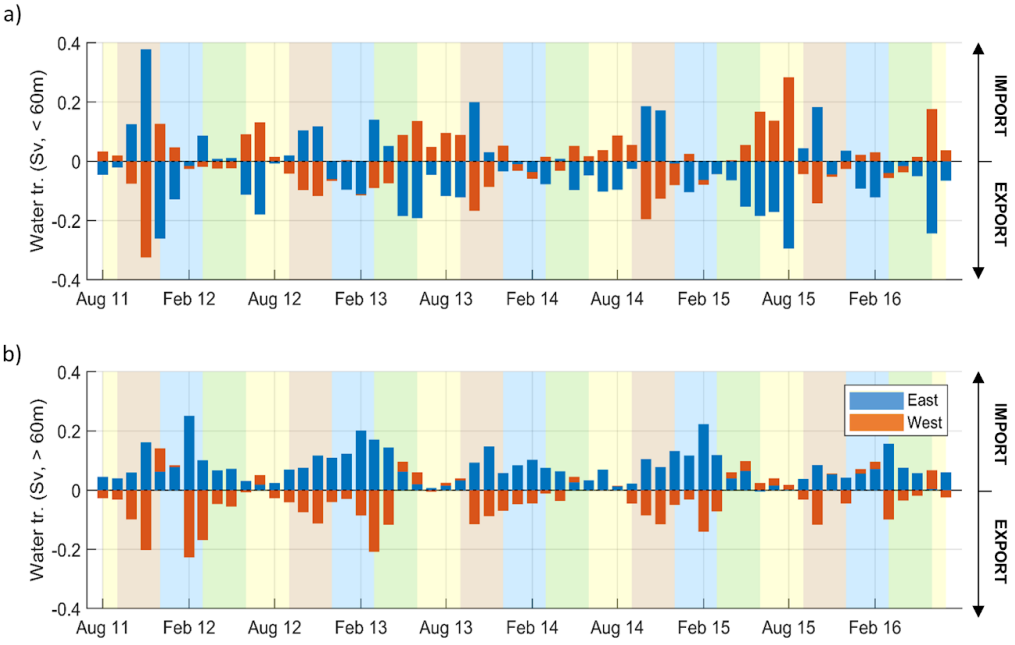

Figure 7: a) Time series for the five simulated years of monthly water transport in the eastern and western part of the shelf (in Sv. - by convention export off the shelf is shown by negative values and the shelf boundaries are indicated in Fig. 1) at the surface (< 60 m depth). Shaded areas show the different seasons over the period simulated (yellow (JJA), brown (SON), blue (DJF), green (MAM)). b) same as a) but for depths superior to 60 m.

4.1.2 Nutrients and phytoplankton

External inputs of inorganic nutrients - Cross-shelf transport of NO_3 (similar results are observed for PO_4 and are not shown) computed along the GoL shelf boundary (the boundary is indicated in Fig. 1) shows the import of nutrients all year round from adjacent seas ($22.8 \pm 2.3\ 10^4$ tN yr^{-1} and $2.92 \pm 0.30\ 10^4$ tP yr^{-1}) (see yellow lines in Fig. 8 and details in Table 1). Nutrients were mainly imported from offshore through the deep layer on the eastern part of the shelf and all year round (Fig. 8b) with a maximum in fall and winter (4-6 10^4 tN $month^{-1}$), especially in 2012, 2013, and 2015. These imports in the deep layer of the shelf were much stronger than the exports which took place mainly in fall and winter and to the west while they were almost nil in spring and summer. In the surface layer, imports and exports were low all year round except in winter for export, which then was of the same order or even higher than in the deep layer. Besides, strong inputs from rivers took place in fall, winter, and spring (not shown). The Rhône inputs represented 95/96 % of the total river inputs. Nitrate river inputs are estimated to $7.1 \pm 1.3\ 10^4$ tN yr^{-1} with maximum values in 2012-2013 (Table 1). Phosphate river inputs are estimated to $0.19 \pm 0.04\ 10^4$ tP yr^{-1} (max. in 2012-2013, Table 1).

https://doi.org/10.5194/bg-2021-82
Preprint. Discussion started: 6 April 2021

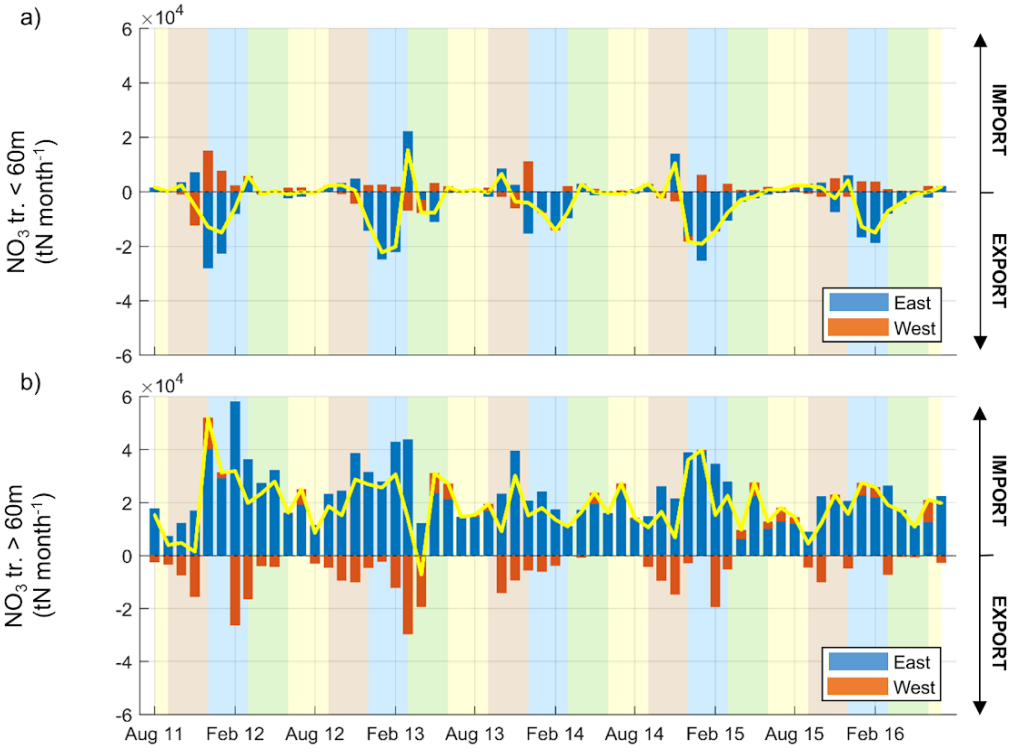

Figure 8: a) Temporal variability of the monthly net surface (depths < 60 m) transport of NO_3 (tN month^{-1}) through the sections defined in Fig. 1. By convention import (export) of NO_3 is shown by positive (negative) values. The residual net transport is shown by the yellow line. Shaded areas show the different seasons over the period simulated (yellow (JJA), brown (SON), blue (DJF), green (MAM)). b) same as a) but for depths >60 m.

https://doi.org/10.5194/bg-2021-82
Preprint. Discussion started: 6 April 2021

Table 1: Mean annual nutrients stock (10^4 tN and tP) and external inputs (10^4 tN and tP yr^{-1}) from the rivers (% of the Rhône is detailed) and from offshore (by convention positive values show an import of nutrients).

	2011-2012	2012-2013	2013-2014	2014-2015	2015-2016	MEAN	SD
NO_3 stock	1.9	2.6	2.3	2.1	2.0	2.2	0.3
NO_3 rivers input (%Rhône)	5.8 (97)	9.2 (96)	7.2 (96)	6.6 (94)	6.5 (98)	7.1 (96)	1.3
NO_3 transport from adjacent seas	26.6	22.8	22.6	20.6	21.6	22.8	2.3
PO_4 stock	0.15	0.18	0.16	0.14	0.13	0.15	0.02
PO_4 rivers input (%Rhône)	0.15 (95)	0.25 (95)	0.20 (96)	0.18 (93)	0.15 (96)	0.19 (95)	0.04
PO_4 transport from adjacent seas	3.39	2.98	2.91	2.66	2.64	2.92	0.30

Stocks over the shelf - Figures 9a-c show the annual cycle of nutrient and phytoplankton stocks integrated over the water column on the Gulf of Lion shelf (bathymetry < 120m) and for the 5 years studied. Figures 9d-f show the annual cycle of the nutrient and chlorophyll profiles averaged on the Gulf of Lion shelf and over the period 2011-2016. The NO_3 stock over the shelf showed a mean annual value of 2.2 10^4 tN and 14% of inter-annual variability. Regarding the PO_4 stock, the shelf showed a mean annual value of 0.15 10^4 tP and 13% of inter-annual variability (Table 1). The nutrient stock was minimum in summer during the stratified period (Fig. 9a-b). The upper layer was depleted in nutrients and the nutriclines were located at ~ 60 m depth (Fig. 9d-e). A deep chlorophyll maximum (DCM) with concentrations of 0.5 mg m^3 was present between 40 and 60 m depth (Fig. 9f). From September onwards, events of vertical mixing associated with northerly gales led to injections of nutrients into the upper layer through the nutricline (Fig. 9a-b) and erosion of the DCM.

In November/December, nutrient stocks increased sharply (Fig. 9a-b) and nutrient profiles became homogeneous over the water column (Fig. 9d-e). Nutrient stocks reached their maximum between the end of December and February when a significant inter-annual variation is found. During this winter period with minimal solar radiation (Fig. 6a), the vertical mixing drove the phytoplankton cells downward where the light intensity was low (Fig. 9f). The phytoplankton biomass was then minimal (Fig. 9c). Superimposed on this seasonal feature, at the monthly scale, significant decreases in chlorophyll stocks were observed in some years in November and December, clearly linked to periods of low solar radiation. From February onwards, as solar radiation increased again, the model predicted a strong increase in phytoplankton biomass in the upper layer

https://doi.org/10.5194/bg-2021-82
Preprint. Discussion started: 6 April 2021

and a decrease in nutrient stocks. The chlorophyll concentration became maximum in March/April (value between 0.8 and 1.3 mg m^{-3}) when the water column restratified (Fig. 9f). In April, DCM reformed when nutrients began to be depleted in the surface layer. It gradually deepened with the deepening of the nutriclines. The phytoplankton biomass decreased.

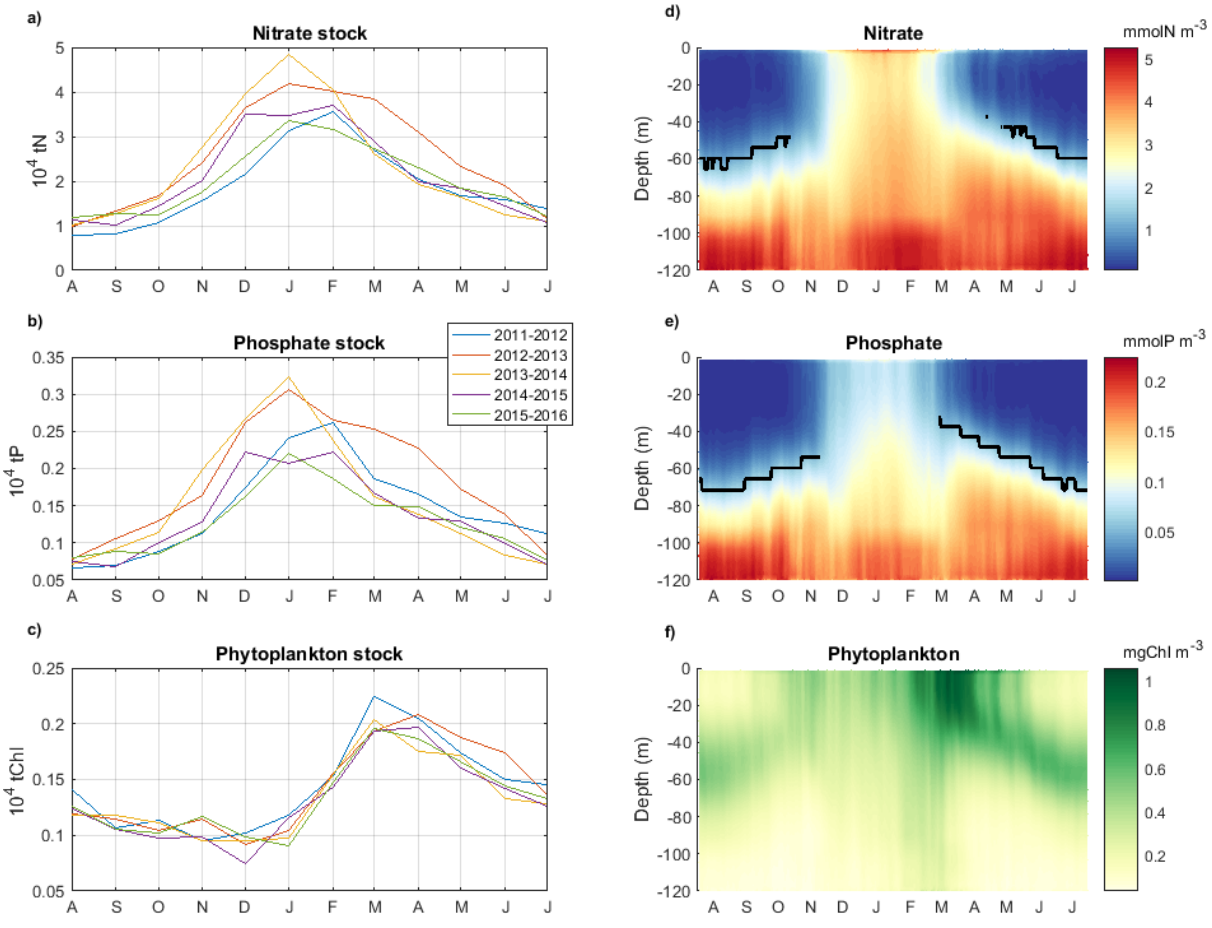

Figure 9: Time series for the five simulated years of depth-integrated monthly averaged stock of a) nitrate (10^4 tN), b) phosphate (10^4 tP), c) chlorophyll (10^4 tChl), and for climatological vertical section of daily concentrations of d) nitrate (mmolN m^{-3}), e) phosphate (mmolP m^{-3}) and f) chlorophyll (mgChl m^{-3}). Black lines on panels E and F represent nutriclines (1 mmolN m^{-3} and 0.05 mmolP m^{-3}).

https://doi.org/10.5194/bg-2021-82
Preprint. Discussion started: 6 April 2021

4.1.3 POC fluxes

The time series of the simulated monthly POC fluxes for the five years is shown in Fig. 10 (spatially integrated over the GoL shelf). Related annual estimates of physical (cross-shelf transport and deposition) and biogeochemical POC fluxes are synthesized in Table 2. GPP (gross primary production) was maximum during spring and summer (~15000 tC day^{-1}) and decreased in winter (~5000 tC day^{-1}) (Fig. 10a). A highly significant correlation of 0.87 ($p<0.01$) is found between GPP and solar radiation. The increase in solar radiation yielded the onset of the late winter/spring GPP (Fig. 10a). Overall, we estimate to 402.8 ± 5.0 10^4 tC yr^{-1} the POC produced through the GPP at the scale of the shelf.

The total respiration, which corresponds to the transformation of POC and DOC to dissolved inorganic carbon (DIC) by phytoplankton, zooplankton, and bacteria, followed the pattern of the GPP with maximum values during late spring and summer (Fig. 10b). In detail, autotrophic respiration, in addition to the exudation to DOC, led to a quantity of POC degraded or recycled in the water column by the producers of about 207.2 ± 6.6 10^4 tC yr^{-1} (51% of the GPP). This entailed a net primary production (NPP) of 195.6 ± 8.2 10^4 tC yr^{-1}. The NPP followed the same patterns during all years with minimum productivity in winter (~3000 tC day^{-1}) and maximum during bloom onset in spring (~8000 tC day^{-1} maximum in April 2012 and June 2013) (Fig. 10e). Besides, 226.5 ± 5.5 10^4 tC yr^{-1} of OC were remineralized by the heterotrophic respiration (79% from bacteria activity). The net metabolism, i.e. the Net Ecosystem Production (NEP, Fig. 10c), which is the difference between the GPP and the community respiration, shows that the ecosystem was productive overall, with NEP estimates of about 89.3 ± 3.3 10^4 tC yr^{-1} at the scale of the shelf (Table 2).

POC fluxes from river inputs were highly variable in time and mainly related to floods of the Rhône River, which locally brought more than 5000 tC day^{-1} during episodic events (Fig. 10d). Overall, it yielded a quantity of POC delivered from rivers of about 13.6 ± 9.8 10^4 tC yr^{-1} with a large inter-annual variability of 72%.

Cross-shelf transport of POC computed along the GoL shelf boundary (Fig. 10f) was highly variable in time and oriented off the GoL shelf with maximum values in winter and spring (max. export of 2000 tC d^{-1} in May 2012, March, and June 2013). During summer and fall, the net transport was weaker. Annually, this led to a net total value of about 24.0 ± 4.2 10^4 tC yr^{-1} of POC exported towards the open sea and the Catalan margin (see details in 4.4).

At last, POC fluxes from the rivers and the biological activity highly contributed to POC deposition over the shelf (Fig. 10g, correlation of R = 0.53 and R = 0.52 ($p<0.001$), respectively). The five years show the role of the NPP on the temporal background with POC deposition between 400 and 800 tC day^{-1} over the shelf. Besides, episodic inputs from rivers during floods increased POC deposition to more than 800 tC day^{-1} at the scale of the shelf in May and June 2013. The different contributions to the POC deposit led to a total of about 19.3 ± 1.2 10^4 tC yr^{-1}.

https://doi.org/10.5194/bg-2021-82
Preprint. Discussion started: 6 April 2021

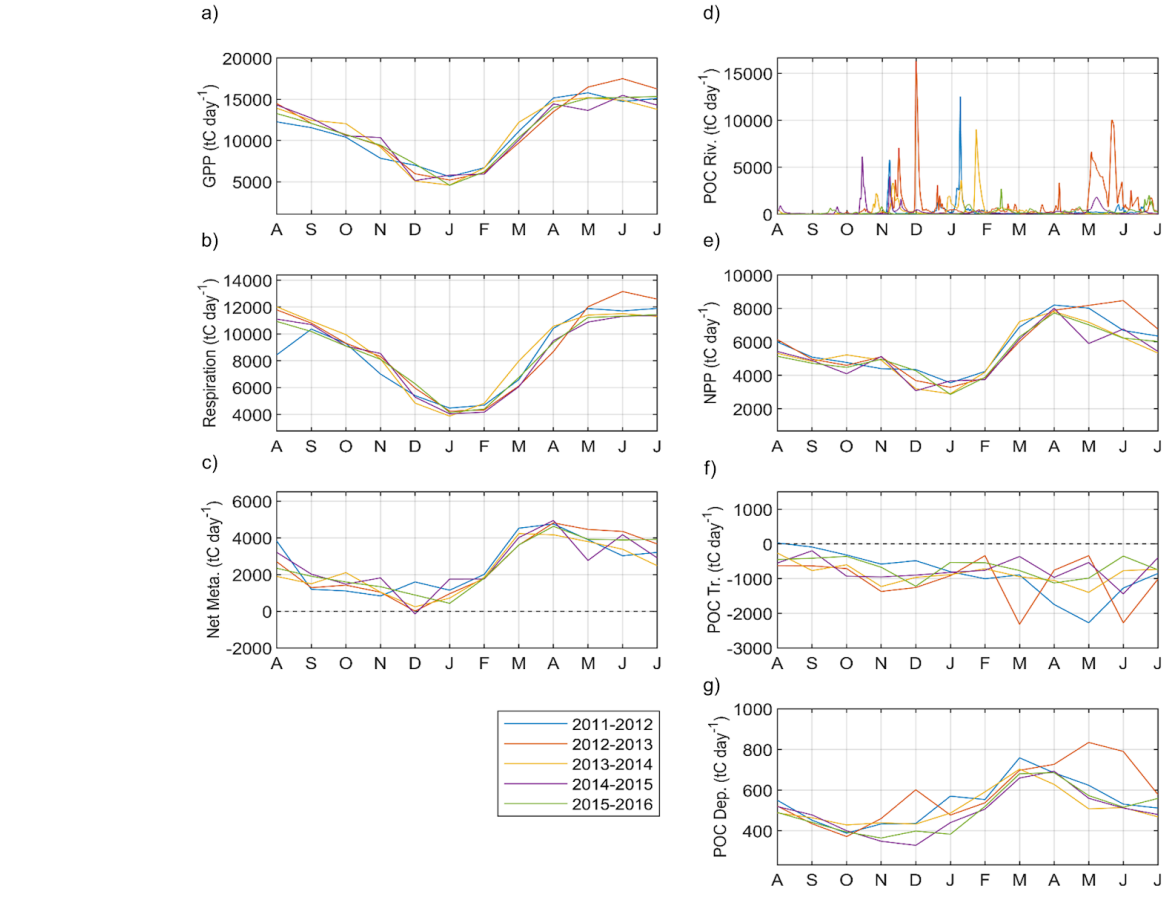

Figure 10: Time series for the five simulated years of POC fluxes (in tC day^{-1}) from a) monthly gross primary production, b) monthly total respiration, c) monthly net metabolism (NEP), d) daily rivers input, e) monthly net primary production, f) monthly transport across the shelf boundary, and g) monthly deposition.

https://doi.org/10.5194/bg-2021-82
Preprint. Discussion started: 6 April 2021

Table 2: Annual POC budget (stock in 10^4 tC and fluxes in 10^4 tC yr^{-1}) of the Gulf of Lion shelf. Cross-shelf net transport across the shelf boundary (indicated in Fig. 1) is specified. By convention net transport off the shelf is shown by a negative value.

	2011-2012	2012-2013	2013-2014	2014-2015	2015-2016	MEAN	SD
Stock POC	7.9	8.0	7.7	7.3	7.5	7.7	0.3
GPP	405.8	409.1	404.0	394.3	401.0	402.8	5.0
Exudation to DOC	109.2	115.0	125.5	126.6	125.1	120.3	7.8
NPP	206.7	203.4	192.3	184.8	190.4	195.6	8.2
Total Respiration	312.9	322.1	319.0	304.0	309.5	313.5	7.3
NEP	92.9	87.0	85.0	90.3	91.5	89.3	3.3
Rivers (% Rhône)	9.1 (96)	30.8 (98)	12.4 (97)	8.6 (94)	7.0 (97)	13.6 (97)	9.8
Deposition	20.0	21.2	18.8	18.1	18.4	19.3	1.2
Remineralisation$_{Sed}$	11.5	14.1	14.5	13.8	13.7	13.5	1.2
Buried$_{Sed}$	8.5	7.1	4.3	4.3	4.7	5.8	1.9
Cross-shelf net transport	-25.7	-30.0	-24.4	-21.0	-19.2	-24.0	4.2

4.2 Spatial variability of the annual NPP over the shelf and interannual variability

The vertically integrated NPP for the 2011-2016 period simulated is presented in Fig. 11. The NPP was not uniform over the shelf. Minima were located along the coast for depth lower than 50 m and showed values in the range of 50-100 gC m^{-2} yr^{-1}. Further offshore, the NPP increased to 150-200 gC m^{-2} yr^{-1} all over the shelf with maximum values close to the shelf break

https://doi.org/10.5194/bg-2021-82
Preprint. Discussion started: 6 April 2021

(120m depth, ~200 gC m^{-2} yr^{-1}). While a trend exists between the NPP and the depth, local maxima were located at the eastern entrance of the shelf and in front of the Rhône mouth with values of approx. 250 gC m^{-2} yr^{-1} in the ROFI (Region Of Freshwater Influence).

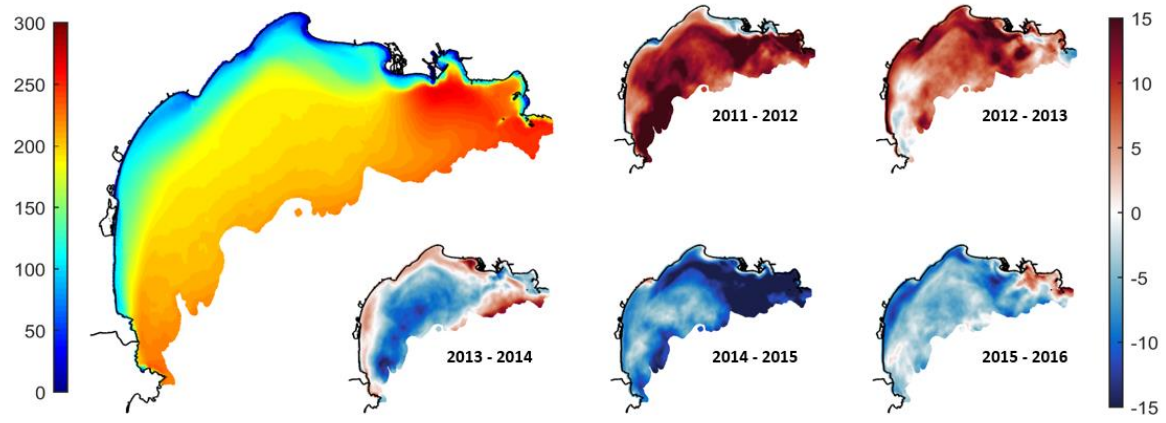

Figure 11: Left: Vertically integrated net primary production (in gC m^{-2} yr^{-1}) averaged over the 2011-2016 period. Right: Annual anomalies in the vertically integrated NPP (in gC m^{-2} yr^{-1}).

The annual anomalies (Fig. 11) show that the first two years (2011-2012 and 2012-2013) of the simulation were more productive than the rest of the simulated years with mean NPP anomalies of +9 gC m^{-2} yr^{-1}. Conversely, the 2013-2016 period showed a lower NPP with mean anomalies of -7 gC m^{-2} yr^{-1}. In detail, our results show that there are maximum anomalies in particular areas of the Gulf of Lion, namely inside the Rhone ROFI, along the coast, and over the southwestern external part of the shelf.

4.3 Spatial variability of the annual POC deposition over the shelf

The POC deposition over the shelf averaged over the 5 years simulated and its annual anomalies are presented in Fig. 12. Our estimates yielded an averaged POC deposition of 19.3 gC m^{-2} yr^{-1}. As for the NPP, the deposition of POC was not uniform over the shelf. It was maximum in front of the river mouths, in particular the Rhône river mouth, with values of about 30 gC m^{-2} yr^{-1}. The POC deposit decreased from 20 gC m^{-2} yr^{-1} in the middle of the shelf, between 20 and 60 m depth, to 10 gC m^{-2} yr^{-1} at the shelf break.

The annual anomalies (Fig. 12) show that during the first two years (2011-2012 and 2012-2013) of the simulation POC deposition was higher than the rest of the simulation with mean anomalies of +0.9 and +0.3 gC m^{-2} yr^{-1}. Conversely, the 2013-

https://doi.org/10.5194/bg-2021-82
Preprint. Discussion started: 6 April 2021

2016 period showed a lower POC deposition with a mean anomaly of -0.5 gC m^{-2} yr^{-1}. In detail, the model shows that there were maximum anomalies in particular areas of the Gulf of Lion shelf, namely over the Rhone prodelta, along the coast for depth lower than 50 m, and to a lesser extent on the central area of the shelf.

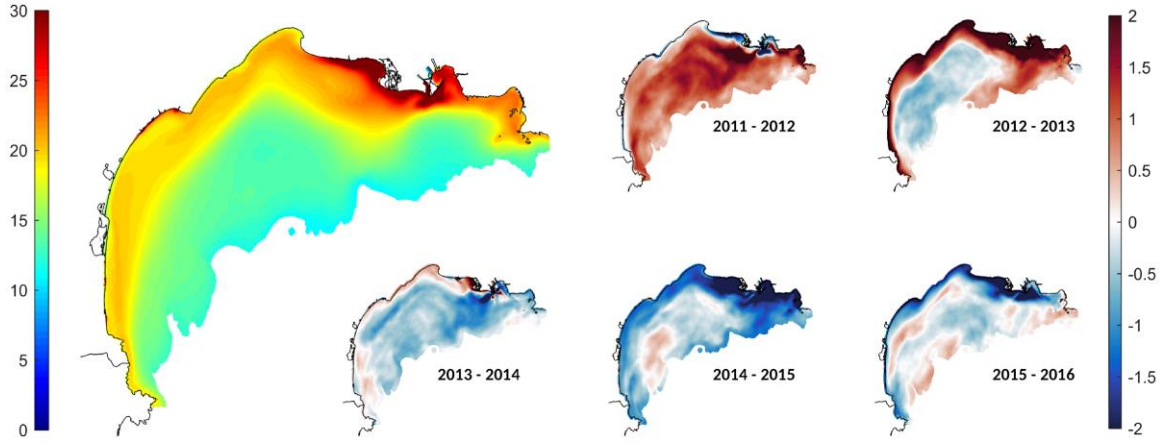

Figure 12: Left: Mean POC deposition over the shelf (in gC m^{-2} yr^{-1}) for the 2011-2016 period. Right: Annual anomalies in the POC deposition (in gC m^{-2} yr^{-1}).

4.4 Cross-shelf transport of POC

Over the 2011-2016 period, the annual net POC transport off the shelf was estimated to 24.0 10^4 tC yr^{-1}. We detailed the transport through different sections of the GoL shelf boundary shown in Fig. 13.

Results highlight the preferential area of the southwestern part of the Gulf of Lion shelf (approx. 10% of the total boundary), which corresponded to 37% of the total POC net transport off the shelf considering the whole water column (8.9 10^4 tC yr^{-1}). Within this western section, the transport was carried out mainly through the Cap de Creus Canyon (CC in Fig. 13, 18% of the total export) and towards the Catalan shelf to the south of the GoL (CS in Fig. 13, 19% of the total export). Besides, our results also show the balanced net transport in the Lacaze-Duthiers canyon (LD in Fig. 13).

Considering only surface waters (0-60 m depth), the POC net transport, oriented towards the open sea and adjacent shelf, amounted to 13.6 10^4 tC yr^{-1}, 57% of the total export, and mainly occurred in the eastern and central parts of the shelf.

https://doi.org/10.5194/bg-2021-82
Preprint. Discussion started: 6 April 2021

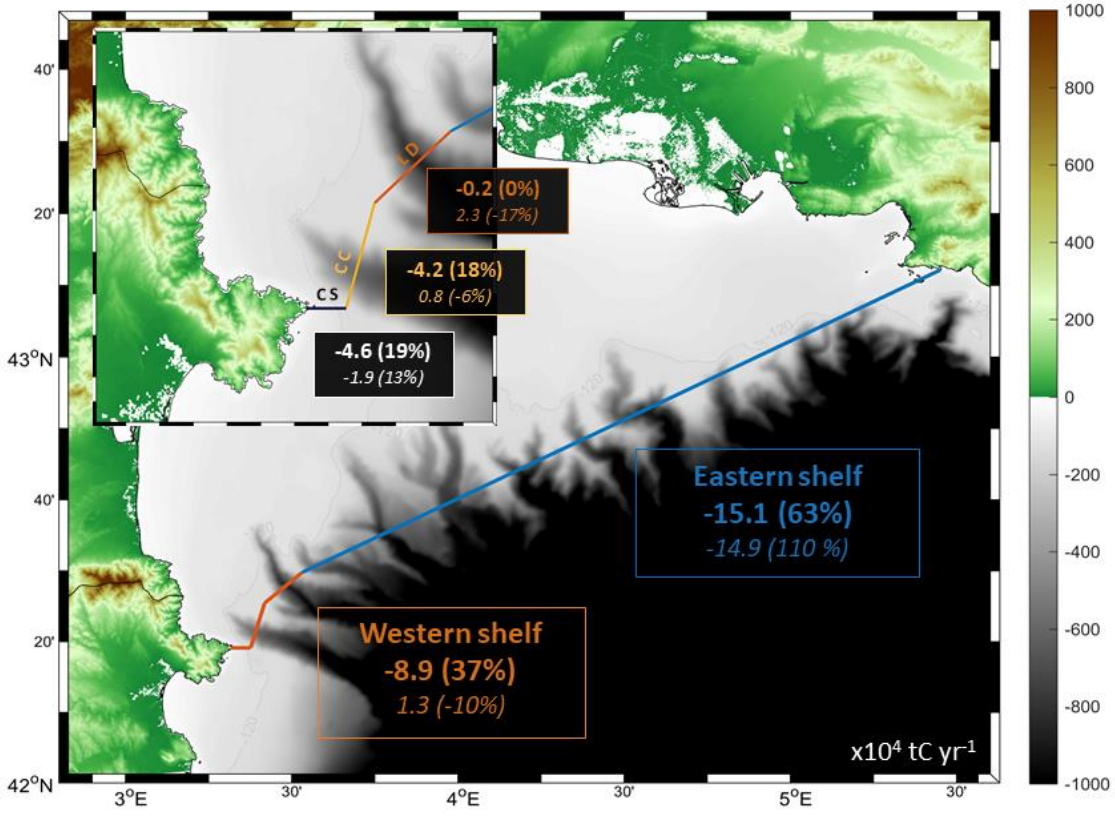

Figure 13: Map of the Gulf of Lion's topography (m) showing the position of the different sections used to describe the POC net transport (10^4 tC yr^{-1}) in the vicinity of the Gulf of Lion slope and at the eastern and western shelf extremities. By convention net transport off the shelf is shown by a negative value. The detail of the western shelf net transport is shown on the top left corner of the map. Note that here the western section is separated into 3 subsections. The bold numbers show the net transport vertically integrated over the water column. The numbers in italics show the surface POC net transport (<60 m depth).

The temporal variability of the POC net transport is shown in Fig. 14. The results show the variability of the export of POC to the open sea through the surface layer (Fig. 14a, <60m depth) or the bottom layer (Fig. 14b, >60m depth). They also show the opposite functioning between the eastern and western parts of the shelf, and in both layers, as in water exchanges.

In the surface layer (Fig. 14a), the overall net transport (yellow line) was in the range of 0-0.5 10^5 tC $month^{-1}$ oriented towards the open sea. Exports occurred mainly in the eastern part of the shelf. They reached maximum values in springs (1.1 10^5 tC $month^{-1}$ during May 2013) with low values in winter and moderate in summer (~0.3 10^5 tC $month^{-1}$). The imports occurred mainly at the end of spring and in summer in the west. They were minimum in winter and occurred episodically in falls in the eastern part of the shelf (maximum in November 2011).

https://doi.org/10.5194/bg-2021-82
Preprint. Discussion started: 6 April 2021

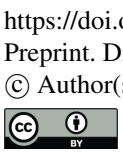

In the bottom layer (Fig. 14b), the overall net transport was lower than in the surface layer with residual export in fall and winter and episodic imports without seasonality. Exports occurred mainly in the western part of the shelf. They reached maximum values in winters 2012, 2013, 2015 (maximum of ~0.4 10^5 tC month^{-1}), and also in falls with slightly lower values. During spring and summer, deep imports of POC in the west occurred, slightly compensated by deep exports in the east.

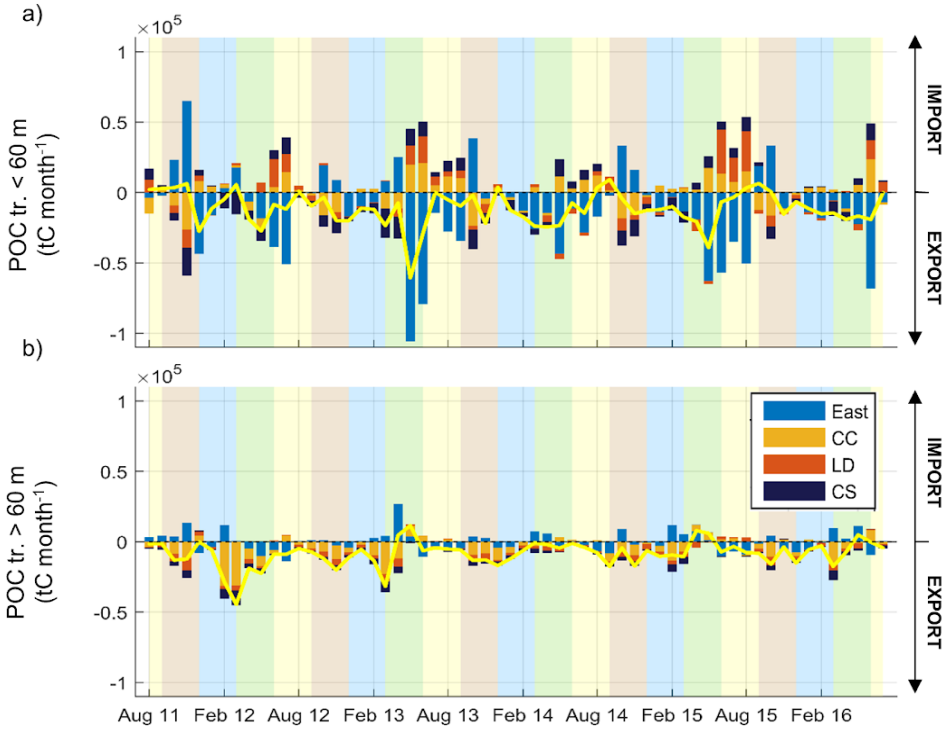

Figure 14: a) Temporal variability of the monthly net surface (< 60m) transport of POC (tC month^{-1}) through the sections defined in Fig. 13. b) same as a) but for depths superior to 60m. Note that here the western section is separated into 3 subsections. By convention import (export) of POC is shown by positive (negative) values. The residual net transport is shown by the yellow line. Shaded areas show the different seasons over the period simulated (yellow (JJA), brown (SON), blue (DJF), green (MAM)).

5. Discussion

A first multi-year assessment with a 3D coupled hydrodynamic-biogeochemical model was presented to quantify POC fluxes on the Gulf of Lion shelf. The model reproduces well the annual cycle of nutrient and phytoplankton concentrations in the Gulf of Lion shelf. The coupling of hydrodynamic-biogeochemical models highlights the role of physical processes as stratification and winter mixing, which impact nutrients dynamics in the upper layer in agreement with previous observational (Diaz et al., 2000) and modelling studies (Tusseau-Vuillemin et al., 1998; Herrmann et al., 2013) in the NW Mediterranean

https://doi.org/10.5194/bg-2021-82
Preprint. Discussion started: 6 April 2021

region. Dynamics in phytoplankton biomass are then well represented through the spring bloom, the summer DCM, and the erosion of the DCM in fall, related to the stratification and nutricline dynamics.

5.1 Annual cycle of nutrients and physical forcings

We have highlighted the year-round import of nutrients on the shelf from offshore waters of about 22 10^4 tN yr^{-1} for nitrate and 3 10^4 tP yr^{-1} for phosphate that represent 3 and 15 times more, respectively, than annual Rhône inputs (7 10^4 tN yr^{-1} - 0.2 10^4 tP yr^{-1}), the difference between nitrate and phosphate being explained by the very high N:P ratio in Rhone river inputs (approx. 80). Minimal values estimated in summer can be attributed to weak water exchanges in the deeper layer at this season (Fig. 7). In fall, exchanges increase (>20 000 tN $month^{-1}$; 2500 tP $month^{-1}$) as water exchanges take place on a thicker layer including the nutricline (Fig. 7-9). Most often these events correspond to fall marine storms. It seems that they can also be partly attributed to the rapid increase in the transport of the Northern Current in November, which corresponds to the activation of its East Corsica branch (Carret et al., 2019). This increase would favor intrusions of the Northern Current on the shelf. Autumn is the beginning of the period also including winter during which the nutrient stocks increase by a factor of 2 to 3 partly due to the low consumption associated with the low solar radiation. Besides, the first two winters were also marked by significant net imports of nutrients on the shelf from February to April 2012 and March 2013. Winter 2012 was marked by extremely dense shelf water formations followed by intense cascading in the canyon of Cap de Creus (Durrieu de Madron et al., 2013). However, as shown in Fig. 7-8, the export of nutrients through dense shelf water cascading in the south-western region was exceeded by nutrient inputs in the eastern part of the shelf where about 30 000 tN $month^{-1}$ were advected for 3 months (February-April 2012). In March 2013, the strong nutrient input corresponds to the interaction between offshore convection, which produced high nutrient concentrations throughout the open-sea water column (nitrate concentration up to 8 µmol L^{-1} near the surface vs. 3 µmol L^{-1} over the shelf, see Kessouri et al. (2017)), and a strong easterly storm that advected these nutrients onto the shelf through the surface and deep layers. Our results are consistent with the results of the modeling study by Tusseau-Vuillemin et al. (1998) who showed such export through dense water cascading, as well as shelf enrichment with nutrients advected from the open-sea convection area.

Throughout the year, it is remarkable that all the physical processes described here, whether they correspond to water input from the eastern or western part of the shelf, at the surface, or in the deep layer, result in a net import of nutrients to the Gulf of Lion shelf. This reveals a systematic consumption of nutrients during the transit of the water masses on the shelf, the water leaving the shelf being poorer than the incoming water. The Gulf of Lion shelf is therefore generally a reactor that consumes the nutrients imported from the open sea all year round to produce planktonic biomass. In more detail, since nutrients are imported mainly under the nutricline, they probably play a major role in stratified periods (summer and autumn) sustaining the production in the DCM and feeding upwelling at the coast. In contrast, in winter, despite high nutrient inputs from the open ocean, the ecosystem is less productive due to low solar radiation and vertical mixing that further reduces the exposure of cells to light. During this season, the dynamics of the shelf linked to the strong winds, combining vertical mixing and Ekman

https://doi.org/10.5194/bg-2021-82
Preprint. Discussion started: 6 April 2021

transport towards the open sea, leads to a vertical circulation of nutrients that enter through the bottom and exit through the surface layer, generally with little benefit for the ecosystem.

The primary production is thus impacted by the nutrient availability in the photic layer imported not only from local bottom waters by vertical mixing or by the rivers but also and importantly from offshore waters, particularly from the Northern Current and even from the deep convection region through marine storms induced circulations (Conan et al., 1998; Tusseau-Vuillemin et al., 1998).

5.2 Biological production

Considering a shelf area of approx. 10 000 km^2, we estimate an averaged NPP of 196 gC m^{-2} yr^{-1}. This result is in line with previous studies in the NW Mediterranean that estimated an annual NPP in the range of 80-150 gC m^{-2} yr^{-1} using local and punctual in situ measurements (Cruzado et Velasquez, 1990; Lefevre et al., 1997; Conan et al., 1998; Durrieu de Madron et al., 2000), or the range of 160-300 gC m^{-2} yr^{-1} from remote sensing (Bosc et al., 2004; Olita et al., 2011), or of 75-250 gC m^{-2} yr^{-1} using biogeochemical models (Lazzari et al. 2012; Teruzzi et al. 2018). Our estimates are also in the upper range of NPP observed over shelves in mid-latitude areas as in the Bering Sea, the North Sea, and the Mid-Atlantic Bight (100-150 gC m^{-2} yr^{-1}, see details in Hofmann et al. (2011)).

The high productivity and the recycling of organic matter during the year were highlighted. Positive NEP values all year round (max. NEP of ~5000 tC d^{-1} during April 2015) show that the GoL shelf acted as a sink of DIC (source of organic carbon) regarding the pelagic planktonic ecosystem (i.e. the biological term). Besides, the NEP decreased during fall and was minimum in winter due to the decrease of the GPP while the total respiration recycled the OC. Negative daily NEP values (not shown) occurred in December 2012 and 2014, and in November 2013, which shows that the GoL shelf ecosystem episodically acted as a source of DIC (Sempéré et al., 2000). Our annual estimate of $89.3 \pm 3.3\ 10^4$ tC yr^{-1} is 43% higher than the estimate of Sempéré et al. (2000).

Primary production at the annual scale shows a weak interannual variation with a standard deviation of 4%. It shows a strong spatial variability with a range from 50 gC m^{-2} yr^{-1} in the very shallow regions, to 200 gC m^{-2} yr^{-1} on the outer shelf and 250 gC m^{-2} yr^{-1} in the eastern part of the shelf. The main spatial variability with a coast-open sea gradient is caused by the increasing reservoir of available nutrients with depth. This spatial pattern is consistent with the study of Macias et al. (2018) showing maximal primary productivity in the deeper and eastern regions of the shelf. Along with this general pattern, changes in environmental variables are expected to play a role in the changes in the NPP over the shelf. Hence, we aim at identifying the key biogeochemical, hydrodynamic, and atmospheric indicators, which could potentially explain the additional spatiotemporal variability in NPP over the simulated period. To that end, we determined the Empirical Orthogonal Functions (EOFs) decomposition and the major Principal Components (PCs) of NPP weekly anomalies (Fig. 15) (see detail in Olita et al. (2011) and Daewel and Schrum (2017)).

https://doi.org/10.5194/bg-2021-82
Preprint. Discussion started: 6 April 2021

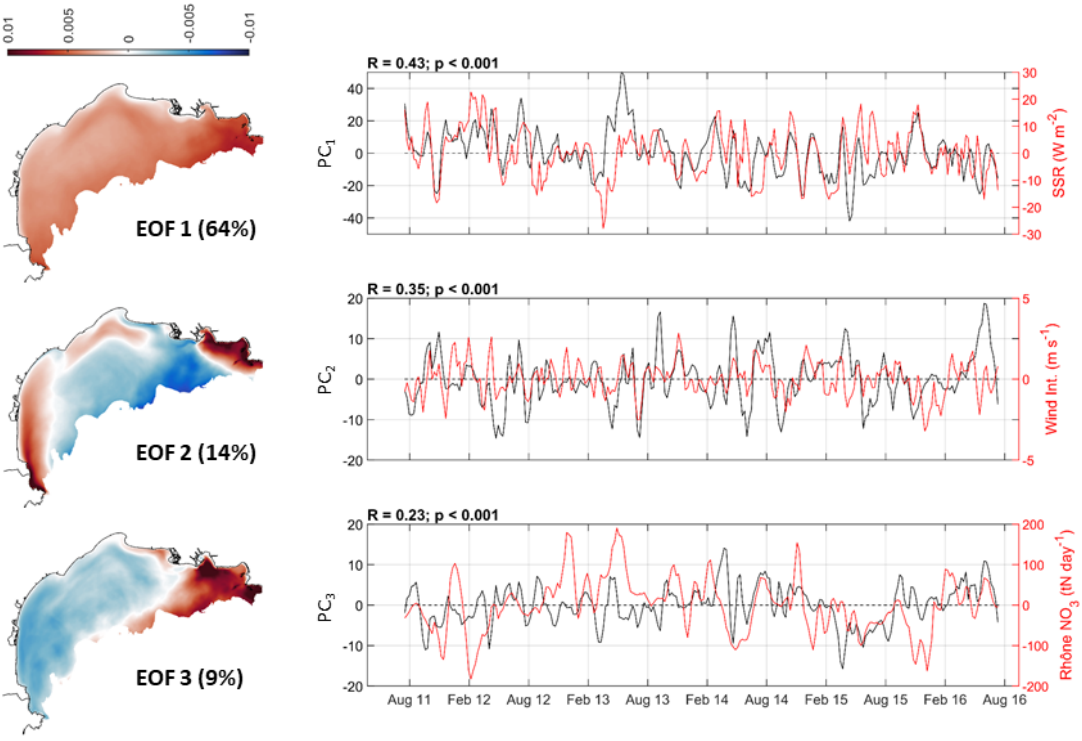

Figure 15: Left: The first 3 empirical orthogonal functions (EOF) for the weekly anomalies of NPP in the Gulf of Lion. Right: Principal components for the pattern of the first 3 EOFs (black). Each PC is related to the weekly anomalies of the related indicator (red); from top to bottom: the solar radiation, the wind intensity, and the Rhône NO_3 input. Weekly anomalies are estimated by subtracting the average annual cycle for each simulated year. A 3-week smooth filter is then applied.

The first EOF explains 64% of the NPP variability with positive values over the entire shelf, and higher values in the eastern region, and along the continental slope. Its temporal variability (PC_1) follows the pattern of the temporal variability of the solar radiation with a correlation of 0.43 ($p<0.001$) (Fig. 15). Besides, the second EOF explains 14% of the NPP changes with an opposite behavior between the coastal area (<50m deep, mainly in the Bay of Marseille and the SW part of the GoL) and the central part of the shelf (see Fig. 15). Its temporal variability (PC_2) is significantly correlated with the weekly anomalies of wind intensity. At last, the third EOF explains 9% of the NPP changes with the opposite behavior between the Rhône ROFI and the rest of the shelf. It is related to the temporal variability of the Rhône river NO_3 anomalies (PC_3, see Fig. 15 - bottom panel, same results are observed with PO_4 anomalies). PCs are thus related to processes that drive the nutrients concentrations, controlling the primary production:

https://doi.org/10.5194/bg-2021-82
Preprint. Discussion started: 6 April 2021

- EOF_1/PC_1: changes in NPP over the entire shelf are positively correlated to solar radiation. This indicates that the primary production over the shelf is controlled by the nutrients available on one hand (see 5.1), and regulated by the anomalies of solar radiation (i.e. light intensity). Maximum production periods thus occur when inputs of nutrients are high (from offshore waters or Rhône River) and are concomitant with periods of strong solar radiation positive anomalies (Legendre, 1990).

- EOF_2/PC_2: changes in NPP in the bay of Marseille and along the coast of the GoL are positively correlated to the wind speed. This indicates the role of wind-induced coastal upwellings in the supply of nutrients to the surface layer that locally favors the primary production (Lefevre et al., 1997; Fraysse et al., 2014), and wind-induced eastern storms when the nutrient-rich Rhone plume is pushed towards the coast and flows southwestward (Ulses et al., 2008a) and may in certain cases be diluted towards the east (Gatti et al., 2006).

- EOF_3/PC_3: changes in NPP in the Rhône ROFI are positively correlated with the Rhône nutrient input anomalies (same results with PO_4, not shown). It shows the role of the Rhône floods in the supply of nutrients to the gulf, which locally increases the NPP (Minas and Minas, 1989; Durrieu de Madron et al., 2003).

5.3 The deposition and offshore export of POC

In terms of POC deposition (Fig. 12), the model reproduces the high accumulation rates observed in front of the Rhône mouth (Cathalot et al., 2013). Besides, the cyclonic circulation favors the alongshore dispersion of the terrestrial material from the Rhône River along the 30-50 m isobaths (Got and Aloisi, 1990; Durrieu de Madron et al., 2000). Annual changes can be related to changes in Rhône terrestrial POC inputs to the shelf (minimum inputs in 2011-2012 and maximum inputs in 2012-2013 corresponding to minimum and maximum deposition in front of the Rhône mouth) as well as to the inter-annual variability of the NPP (see above) that drove the deposition of POC over the shelf (max. NPP in 2011-2012) in agreement with Auger et al. (2011). Besides, it is also noteworthy that these results do not take into account possible wave-induced sediment resuspension processes during storms, which participate in changes in sediment deposition areas (Bourrin et al., 2015). The future development of a fully coupled hydrodynamic, sedimentary, and biogeochemical model could provide a better description of the dynamics of POC deposition, in particular on the inner shelf (0-30 m). Among the deposited sediments, the average remineralization rate of POC was estimated to 70% leading to a loss by the degradation of about 13.5 (+/- 1.2) 10^4 tC yr^{-1} in the sediment (Table 2). This result is in line with Accornero et al. (2003) and Pastor et al. (2011), who estimated a mean remineralization rate of 60% in the Gulf of Lion, and with Durrieu de Madron et al. (2000), who estimated a total loss by the degradation of 33.8 (+/- 16.1) 10^4 tC yr^{-1} at the water-sediment interface.

Our results have highlighted the first order of importance of the cyclonic circulation that occurs over the shelf and that favors water and POC export in the southwestern part of the shelf (~2900 tC yr^{-1} km^{-1} across the western boundary compared to ~850 tC yr^{-1} km^{-1} for the eastern one). They agree with the results from previous studies, which showed the important water and particulate matter export in this part of the shelf due to the winter coastal circulation (Estournel et al., 2003; Ulses et al. 2008c)

https://doi.org/10.5194/bg-2021-82
Preprint. Discussion started: 6 April 2021

and episodic marine storm events (Ulses et al., 2008a; 2008b; Bourrin et al., 2015). Lapouyade and Durrieu de Madron (2001) estimated from in-situ measurements a mean transport of 3.3 10^4 tC $month^{-1}$ (12.8 kg s^{-1}) in winter that drastically decreased to 0.2 10^4 tC $month^{-1}$ (0.8 kg s^{-1}) during the summer. These estimates are of the same order as those obtained here, with mean winter and summer POC transport of 2.3 10^4 and 0.5 10^4 tC $month^{-1}$.

The estimates of POC transport for individual parts of the western slope (see Fig. 13) demonstrate the importance of the Cap de Creus Canyon area and the adjacent narrow part of the shelf (CS in Fig. 13) in the export of POC off the GoL (4.2 and 4.6 10^4 tC yr^{-1}, respectively). It is also remarkable that this transport is maximum in winters 2011-2012 and 2012-2013, during a period marked by several cascading events (Durrieu de Madron et al., 2013) and marine storms (Bourrin et al., 2015). Indeed, this part of the shelf is an active area in the export of POC towards the open sea and the deeper environments as highlighted in Puig et al. (2008) and Sanchez-Vidal et al. (2008). Besides, it is noticeable that the Lacaze-Duthiers canyon area shows a balanced net transport of POC with maximum imports in summer 2013 and 2015 and low exports in winters. It probably highlights the balance existing between the inputs from the open sea during the stratified period and continental winds that generate anticyclonic eddies in this area (Estournel et al., 2003; Hu et al., 2011), and outputs from transport during extreme events as storms and dense-shelf waters cascading (Palanques et al., 2006).

We estimate that approx. 4.6 (+/-2.8) 10^4 tC yr^{-1} was exported towards the Catalan margin and the Gulf of Rosas by-passing the Cap de Creus Canyon. This value, which represents approx. 20% of the total net transport off the shelf, shows a significant contribution of POC from the GoL to this area. Future studies could focus on the balance between POC inputs from the southwestern part of the GoL and from local rivers (as Tordera, Ter, and Fluvia rivers), estimated at 0.13 10^4 tC yr^{-1} by Sanchez-Vidal et al. (2013). Observations in this part of the shelf could also validate our estimates in this area, which has been seldom instrumented from now.

Considering surface waters, the impact of the steady northwestern wind that favors offshore water exports through eddies and intrusions of the Northern Current has been identified as the main factor regulating surface shelf-slope exchanges in this area (Estournel et al., 2003; Petrenko, 2003). The surface export of POC is also related to the spread of the Rhône River plume towards the open sea during floods and surface currents favorable conditions (Gangloff et al., 2019; Many et al., 2018). The high concentrations of POC in the plume therefore actively contribute to offshore exports through the Northern Current during these episodic events.

6. Conclusion

A 3D coupled hydrodynamic-biogeochemical model was used to estimate the POC budget of the Gulf of Lion shelf, and to understand the mechanisms responsible for its spatiotemporal variability over the period 2011-2016. The validation of the model was performed using existing data from a multi-platform observation system. A good agreement between model results and observations at different space and time scales was shown. The model represents the high dynamical character of the Gulf

https://doi.org/10.5194/bg-2021-82
Preprint. Discussion started: 6 April 2021

of Lion shelf in terms of hydrodynamic (stratification/winter mixing) and biogeochemical conditions (nutrients, chlorophyll and POC dynamics).

Spatial, seasonal and inter-annual changes in the different POC input and output terms were identified. Model results highlight the high NPP occurring in the GoL shelf (196 10^4 tC yr^{-1}) with maximum values in spring and in the outer shelf, in particular in the eastern region. The interannual variability of the NPP at the Gulf of Lion scale is especially low (SD = 4%) and monthly interannual anomalies in NPP are mainly explained by changes in the intensity of solar radiation. Our results also show that the nutrient enrichment from the general circulation and the open sea (22 10^4 tN yr^{-1} and 3 10^4 tP yr^{-1}), representing on average 3 times for nitrate, and 15 times for phosphate, the inputs from the Rhone, favors the phytoplankton growth over the entire shelf. Coastal upwelling as well as inputs for the Rhone also contribute locally and to a lesser extent to changes in NPP. The positive NEP values during a large part of the year show that the GoL annually acts as a sink of DIC regarding the pelagic planktonic ecosystem.

Rivers contribute to the POC delivery to the shelf with a mean value of 19 10^4 tC yr^{-1} representing 10% of the NPP, and strong changes induced by floods (72% inter-annual variability). At last, we have shown the high dynamical character of the GoL shelf waters, which results in strong cross-shelf transport of POC oriented off-shelf (24 10^4 tC yr^{-1}). Our estimates have shown that 57% of the export occurred in the surface layer through the eastern and central part of the shelf, and 43% below 60 m mostly through the western part of the shelf and favored by marine winds in fall and cascading events in winter.

At the scale of the western Mediterranean Sea, our results show the crucial role of the Gulf of Lion shelf, which acts as a reactor that consumes the inorganic nutrients imported from the open sea to produce organic matter all year round. A part of the produced organic matter is exported by the coastal circulation towards the Catalan shelf and the open sea, yielding to the enrichment in POC of adjacent coastal waters, the Northern Current and the deeper basin. The autotrophic status of the ecosystem along with the highly dynamical character of the area, marked by low residence times and shelf-slope processes as dense shelf water cascading, suggest that the GoL shelf could act as a sink for atmospheric CO_2 and favor carbon sequestration. The future coupling of the model presented in this work with a carbonate system module describing the dynamics of dissolved inorganic carbon and estimating the air-sea CO_2 fluxes could allow a better understanding and a quantification of the source/sink role of atmospheric CO_2 on the shelf.

This work represents the first step for further investigations and quantifications of phenomena such as the impact of climate change on cascading events and bottom export, or the effect of reduced nutrient inputs from coastal rivers.

Acknowledgments

Numerical simulations were performed using the SYMPHONIE model, developed by the SIROCCO group (https://sirocco.obs-mip.fr/) and computed on HPC resources of CALMIP (CALcul en MIdi-Pyrénées, projects 1331, 1325 and 09115) and GENCI (Grand Equipement National de Calcul Intensif, project A0010110088). Datasets were retrieved from

620 the SOMLIT network (Service d'Observation en Milieu Littoral; http://somlit.epoc.u-bordeaux1.fr/fr). We thank the SOERE MOOSE for supporting and providing long-term observation data in the Gulf of Lion. We especially thank the French glider team, P. Testor, and F. Bourrin for their help on the glider data processing.

Financial support

This work was funded by the ANR AMORAD project under the ANR Program (ANR-11-RSNR-0002). The postdoctoral
625 fellowship of Gaël Many was also funded by ANR AMORAD.

References

Accornero, A., Picon, P., De Bovée, F., Charrière, B., and Buscail, R.: Organic carbon budget at the sediment-water interface on the Gulf of Lions continental margin, Cont. Shelf Res., 23, 79-92, https://doi.org/10.1016/S0278-4343(02)00168-1, 2003.

Auger, P. A., Diaz, F., Ulses, C., Estournel, C., Neveux, J., Joux, F., and Naudin, J. J.: Functioning of the planktonic ecosystem
630 on the Gulf of Lions shelf (NW Mediterranean) during spring and its impact on the carbon deposition: a field data and 3-D modelling combined approach, Biogeosciences, 8, 3231-3261, https://doi.org/10.5194/bg-8-3231-2011, 2011.

Bauer, J.E. and Druffel, E.R.M.: Oceans margins as a significant source of organic matter to the deep open ocean, Nature, 392, 482–485, https://doi.org/10.1038/33122, 1998.

Behrenfeld, M. J., Westberry, T. K., Boss, E. S., O'Malley, R. T., Siegel, D. A., Wiggert, J. D., and Moore, J. K.: Satellite-
635 detected fluorescence reveals global physiology of ocean phytoplankton, Biogeosciences, 6, 779-794, https://doi.org/10.5194/bg-6-779-2009, 2009.

Bentsen, M., Evensen, G., Drange, H., and Jenkins, A. D.: Coordinate transformation on a sphere using conformal mapping, Monthly Weather Review, 127, 2733-2740, https://doi.org/10.1175/1520-0493(1999)127<2733:CTOASU>2.0.CO;2, 1999.

Bosc, E., Bricaud, A., and Antoine, D.: Seasonal and interannual variability in algal biomass and primary production in the
640 Mediterranean Sea, as derived from 4 years of SeaWiFS observations, Global Biogeochemical Cycles, 18, https://doi.org/10.1029/2003GB002034, 2004.

Bouffard, J., S. Vignudelli, M. Herrmann, F. Lyard, P. Marsaleix, Y. Ménard, and P. Cipollini.: Comparison of ocean dynamics with a regional circulation model and improved altimetry in the North-western Mediterranean, Terrestrial, Atmospheric and Oceanic Sciences, 19, 117-133, https://doi.org/10.3319/TAO.2008.19.1-2.117(SA), 2008.

645 Bourrin, F., Many, G., Durrieu de Madron, X., Martín, J., Puig, P., Houpert, L., and Béguery, L.: Glider monitoring of shelf suspended particle dynamics and transport during storm and flooding conditions, Cont. Shelf Res., 109, 135-149, https://doi.org/10.1016/j.csr.2015.08.031, 2015.

Briton, F., Cortese, D., Duhaut, T., and Guizien, K.: High-resolution modelling of ocean circulation can reveal retention spots important for biodiversity conservation, Aquatic Conservation: Marine and Freshwater Ecosystems, 28, 882-893, https://doi.org/10.1002/aqc.2901, 2018.

Butenschön, M., Zavatarelli, M., and Vichi, M.: Sensitivity of a marine coupled physical biogeochemical model to time resolution, integration scheme and time splitting method, Ocean Modelling, 52, 36-53, https://doi.org/10.1016/j.ocemod.2012.04.008, 2012.

Carret, A., Birol, F., Estournel, C., Zakardjian, B., and Testor, P.: Synergy between in situ and altimetry data to observe and study Northern Current variations (NW Mediterranean Sea), Ocean Sci., 15, 269-290, https://doi.org/10.5194/os-15-269-2019, 2019.

Cathalot, C., Rabouille, C., Tisnérat-Laborde, N., Toussaint, F., Kerhervé, P., Buscail, R., ... and Lansard, B.: The fate of river organic carbon in coastal areas: a study in the Rhône River delta using multiple isotopic (δ13C, Δ14C) and organic tracers, Geochimica et Cosmochimica Acta, 118, 33-55, https://doi.org/10.1016/j.gca.2013.05.001, 2013.

Conan, P., Pujo-Pay, M., Raimbault, P., and Leveau, M.: Variabilité hydrologique et biologique du golfe du Lion. II. Productivité sur le bord interne du courant, Oceanologica Acta, 21, 767-782, https://doi.org/10.1016/S0399-1784(99)80005-X, 1998.

Cruzado, A., and Velasquez, Z.R.: Nutrients and phytoplankton in the Gulf of Lions, northwestern Mediterranean, Cont. Shelf Res., 10, 931 – 942, https://doi.org/10.1016/0278-4343(90)90068-W, 1990.

Daewel, U., and Schrum, C.: Low-frequency variability in North Sea and Baltic Sea identified through simulations with the 3-D coupled physical–biogeochemical model ECOSMO, Earth System Dynamics, 8, 801-815, https://doi.org/10.5194/esd-8-801-2017, 2017.

Dagg, M., Benner, R., Lohrenz, S., and Lawrence, D.: Transformation of dissolved and particulate materials on continental shelves influenced by large rivers: plume processes, Cont. Shelf Res., 24, 833-858, https://doi.org/10.1016/j.csr.2004.02.003, 2004.

Dagg, M. J., Bianchi, T., McKee, B., and Powell, R.: Fates of dissolved and particulate materials from the Mississippi river immediately after discharge into the northern Gulf of Mexico, USA, during a period of low wind stress, Cont. Shelf Res., 28, 1443-1450, https://doi.org/10.1016/j.csr.2006.12.009, 2008.

Davis, R. E., Eriksen, C. C., and Jones, C. P.: Autonomous buoyancy-driven underwater gliders, The technology and applications of autonomous underwater vehicles, 37-58, 2002.

Diaz, F., Raimbault, P., Conan, P.: Small-scale study of primary productivity during spring in a Mediterranean coastal area (Gulf of Lions), Continental Shelf Research, 20, 975-996, 2000.

Dufau-Julliand, C., Marsaleix, P., Petrenko, A., and Dekeyser, I.: Three-dimensional modeling of the Gulf of Lion's hydrodynamics (northwest Mediterranean) during January 1999 (MOOGLI3 Experiment) and late winter 1999: Western Mediterranean Intermediate Water's (WIW's) formation and its cascading over the shelf break, Journal of Geophysical Research: Oceans, 109, https://doi.org/10.1029/2003JC002019, 2004.

Durrieu de Madron, X., Abassi, A., Heussner, S., Monaco, A., Aloisi, J. C., Radakovitch, O., Giresse, P., Buscail, R., and Kerhervé, P.: Particulate matter and organic carbon budgets for the Gulf of Lions (NW Mediterranean), Oceanologica Acta, 23, 717–730, https://doi.org/10.1016/S0399-1784(00)00119-5, 2000.

Durrieu de Madron, X., Denis, L., Diaz, F., Garcia, N., Guieu, C., Grenz, C., and Ridame, C.: Nutrients and carbon budgets for the Gulf of Lion during the Moogli cruises, Oceanologica Acta, 26, 421-433, https://doi.org/10.1016/S0399-1784(03)00024-0, 2003.

Durrieu de Madron, X., Houpert, L., Puig, P., Sanchez-Vidal, A., Testor, P., Bosse, A., ... and Raimbault, P.: Interaction of dense shelf water cascading and open-sea convection in the northwestern Mediterranean during winter 2012, Geophysical Research Letters, 40, 1379-1385, https://doi.org/10.1002/grl.50331, 2013.

Estournel, C., Auclair, F., Lux, M., Nguyen, C., and Marsaleix, P.: "Scale oriented" embedded modeling of the North-Western Mediterranean in the frame of MFSTEP, Ocean Sci., 5, 73-90, https://doi.org/10.5194/os-5-73-2009, 2009.

Estournel, C., Durrieu de Madron, X., Marsaleix, P., Auclair, F., Julliand, C., and Vehil, R.: Observation and modeling of the winter coastal oceanic circulation in the Gulf of Lion under wind conditions influenced by the continental orography (FETCH experiment), Journal of Geophysical Research: Oceans, 108, https://doi.org/10.1029/2001JC000825, 2003.

Estournel, C., Kondrachoff, V., Marsaleix, P., and Vehil, R.: The plume of the Rhone: numerical simulation and remote sensing, Cont. Shelf Res., 17, 899-924, https://doi.org/10.1016/S0278-4343(96)00064-7, 1997.

Estournel, C., Testor, P., Damien, P., D'Ortenzio, F., Marsaleix, P., Conan, P., and Prieur, L.: High resolution modeling of dense water formation in the north-western Mediterranean during winter 2012–2013: Processes and budget, Journal of Geophysical Research: Oceans, 121, 5367–5392, https://doi.org/10.1002/2016JC011935, 2016.

Fraysse, M., Pairaud, I., Ross, O. N., Faure, V. M., and Pinazo, C.: Intrusion of Rhone River diluted water into the Bay of Marseille: Generation processes and impacts on ecosystem functioning, Journal of Geophysical Research: Oceans, 119, 6535-6556, https://doi.org/10.1002/2014JC010022, 2014.

Fraysse, M., Pinazo, C., Faure, V. M., Fuchs, R., Lazzari, P., Raimbault, P., and Pairaud, I.: Development of a 3D coupled physical-biogeochemical model for the Marseille coastal area (NW Mediterranean Sea): what complexity is required in the coastal zone?, PloS one, 8, https://doi.org/10.1371/journal.pone.0080012, 2013.

Gangloff, A., Verney, R., Doxaran, D., Ody, A., and Estournel, C.: Investigating Rhône River plume (Gulf of Lions, France) dynamics using metrics analysis from the MERIS 300m Ocean Color archive (2002–2012), Cont. Shelf Res., 144, 98-111, https://doi.org/10.1016/j.csr.2017.06.024, 2017.

Gao, S. and Wang, Y. P.: Changes in material fluxes from the Changjiang River and their implications on the adjoining continental shelf ecosystem, Cont. Shelf. Res., 28, 1490–1500, https://doi.org/10.1016/j.csr.2007.02.010, 2008.

Gohin, F.: Annual cycles of chlorophyll-*a*, non-algal suspended particulate matter, and turbidity observed from space and in-situ in coastal waters, Ocean Sci., 7, 705–732, https://doi.org/10.5194/os-7-705-2011, 2011.

Got, H., and Aloisi, J. C.: The Holocene sedimentation on the Gulf of Lions margin: a quantitative approach, Cont. Shelf Res., 10, 841-855, https://doi.org/10.1016/0278-4343(90)90062-Q, 1990.

Herrmann, M., Diaz, F., Estournel, C., Marsaleix, P., and Ulses, C.: Impact of atmospheric and oceanic interannual variability on the Northwestern Mediterranean Sea pelagic planktonic ecosystem and associated carbon cycle, Journal of Geophysical Research: Oceans, 118, 5792-5813, https://doi.org/10.1002/jgrc.20405, 2013.

Hofmann, E. E., Cahill, B., Fennel, K., Friedrichs, M. A., Hyde, K., Lee, C., and Xue, J.: Modeling the dynamics of continental shelf carbon, Annual Review of Marine Science, 3, 93-122, https://doi.org/10.1146/annurev-marine-120709-142740, 2011.

Hu, Z. Y., Petrenko, A. A., Doglioli, A. M., and Dekeyser, I.: Study of a mesoscale anticyclonic eddy in the western part of the Gulf of Lion, Journal of Marine Systems, 88, 3-11, https://doi.org/10.1016/j.jmarsys.2011.02.008, 2011.

Kessouri, F., Ulses, C., Estournel, C., Marsaleix, P., D'Ortenzio, F., Severin, T., and Conan, P.: Vertical mixing effects on phytoplankton dynamics and organic carbon export in the western Mediterranean Sea, Journal of Geophysical Research: Oceans, 123, 1647-1669, https://doi.org/10.1002/2016JC012669, 2018.

Kessouri, F., Ulses, C., Estournel, C., Marsaleix, P., Severin, T., Pujo-Pay, M., and Taillandier, V.: Nitrogen and phosphorus budgets in the Northwestern Mediterranean deep convection region, Journal of Geophysical Research: Oceans, 122, 9429-9454, https://doi.org/10.1002/2016JC012665, 2017.

Lapouyade, A., and Durrieu de Madron, X.: Seasonal variability of the advective transport of particulate matter and organic carbon in the Gulf of Lion (NW Mediterranean), Oceanologica Acta, 24, 295-312, https://doi.org/10.1016/S0399-1784(01)01148-3, 2001.

Large, W. G., and Yeager, S. G.: Diurnal to decadal global forcing for ocean and sea-ice models: The data sets and flux climatologies (NCAR Tech. Note NCAR/TN-4601STR), Boulder, CO: National Center of Atmospheric Research, https://doi.org/10.5065/D6KK98Q6, 2004.

Lazzari, P., Solidoro, C., Ibello, V., Salon, S., Teruzzi, A., Béranger, K., and Crise, A.: Seasonal and inter-annual variability of plankton chlorophyll and primary production in the Mediterranean Sea: a modelling approach, Biogeosciences, 9, 217-233, https://doi.org/10.5194/bg-9-217-2012, 2012.

Lefevre, D., Minas, H.J., Minas, M., Robinson, C., Williams, P.J. Le B., and Woodward, E.M.S.: Review of gross community production, primary production, net community production and dark community respiration in the Gulf of Lion, Deep-Sea Research II, 44, 801–832, https://doi.org/10.1016/S0967-0645(96)00091-4, 1997.

Legendre, L.: The significance of microalgal blooms for fisheries and for the export of particulate organic carbon in oceans, Journal of Plankton Research, 12, 681-699, https://doi.org/10.1093/plankt/12.4.681, 1990.

Lohrenz, S. E., Redalje, D. G., Cai, W. J., Acker, J., and Dagg, M.: A retrospective analysis of nutrients and phytoplankton productivity in the Mississippi River plume, Cont. Shelf. Res., 28, 1466–1475, https://doi.org/10.1016/j.csr.2007.06.019, 2008.

Liénart, C., Savoye, N., Bozec, Y., Breton, E., Conan, P., David, V., Feunteun, E., Grangeré, K., Kerhervé, P., ... and Sultan, E.: Dynamics of particulate organic matter composition in coastal systems: a spatio-temporal study at multi-systems scale. Prog. Oceanogr. 156, 221–239. http://dx.doi.org/10.1016/j.pocean.2017.03.001, 2017.

Liénart, C., Savoye, N.,David, V., Ramond, P., Tress, P. R., Hanquiez, V., Marieu, V., Aubert, F., Aubin, S., Bichon, S., Boinet, C., Bourasseau, L., Bozec, Y., … and Susperregui, N.: Dynamics of particulate organic matter composition in coastal systems: Forcing of spatio-temporal variability at multi-systems scale, Progress in Oceanography, 162, 271-289, https://doi.org/10.1016/j.pocean.2018.02.026, 2018.

Liu, G., and Chai, F.: Seasonal and interannual variability of primary and export production in the South China Sea: a three-dimensional physical-biogeochemical model study, ICES Journal of Marine Science, 66, 420–431, https://doi.org/10.1093/icesjms/fsn219, 2009.

Liu, K.-K., Atkinson, L., Quinones, R., and Talaue-NcManus, L.: Carbon and Nutrient Fluxes in Continental Margins: A Global Synthesis, Springer, Berlin, Germany, https://doi.org/10.1007/978-3-540-92735-8, 2010.

Ludwig, W., Bouwman, A. F., Dumont, E., and Lespinas, F.: Water and nutrient fluxes from major Mediterranean and Black Sea rivers: Past and future trends and their implications for the basin-scale budgets, Global Biogeochemical Cycles, 24, https://doi.org/10.1029/2009GB003594, 2010.

Ludwig, W., Dumont, E., Meybeck, M., and Heussner, S.: River discharges of water and nutrients to the Mediterranean and Black Sea: major drivers for ecosystem changes during past and future decades?, Progress in oceanography, 80, 199-217, https://doi.org/10.1016/j.pocean.2009.02.001, 2009.

Macias, D., Garcia-Gorriz, E. and Stips, A.: Major fertilization sources and mechanisms for Mediterranean Sea coastal ecosystems. Limnol. Oceanogr., 63: 897-914. https://doi.org/10.1002/lno.10677, 2018.

Maillet, G. M., Vella, C., Berné, S., Friend, P. L., Amos, C. L., Fleury, T. J., and Normand, A.: Morphological changes and sedimentary processes induced by the December 2003 flood event at the present mouth of the Grand Rhône River (southern France), Marine Geology, 234, 159-177, https://doi.org/10.1016/j.margeo.2006.09.025, 2006.

Many, G., Bourrin, F., Durrieu de Madron, X., Ody, A., Doxaran, D., and Cauchy, P.: Glider and satellite monitoring of the variability of the suspended particle distribution and size in the Rhône ROFI, Progress in Oceanography, 163, 123-135, https://doi.org/10.1016/j.pocean.2017.05.006, 2018.

Marsaleix, P., Auclair, F., and Estournel, C.: Considerations on Open Boundary Conditions for Regional and Coastal Ocean Models, Journal of Atmospheric and Oceanic Technology, 23, 1604-1613, http://dx.doi.org/10.1175/JTECH1930.1, 2006.

Marsaleix P., Auclair, F., Floor, J. W., Herrmann, M. J., Estournel, C., Pairaud, I., and Ulses, C.: Energy conservation issues in sigma-coordinate free-surface ocean models, Ocean Modelling, 20, 61-89, http://dx.doi.org/10.1016/j.ocemod.2007.07.005, 2008.

Marsaleix, P., Estournel, C., Kondrachoff, V., and Vehil, R.: A numerical study of the formation of the Rhône River plume, Journal of Marine Systems, 14, 99-115. https://doi.org/10.1016/S0924-7963(97)00011-0, 1998.

Minas, M., and Minas, H. J.: Primary production in the Gulf of Lions with considerations to the Rhone River inputs, Water pollution research reports, 13, 112-125, 1989.

Mikolajczak, G., Estournel, C., Ulses, C., Marsaleix, P., Bourrin, F., Martín, J., Pairaud, I., Puig, P., Leredde, Y., Many, G., Seyfried, L., Durrieu de Madron, X.: Impact of storms on residence times and export of coastal waters during a mild autumn/winter period in the Gulf of Lion, Cont. Shelf Res., 207, https://doi.org/10.1016/j.csr.2020.104192, 2020.

Moutin, T., Raimbault, P., Golterman, H. L., and Coste, B.: The input of nutrients by the Rhône River into the Mediterranean Sea: Recent observations and comparison with earlier data, Hydrobiologia, 373, 237, https://doi.org/10.1023/A:1017020818701, 1998.

Naudin, J. J., Cauwet, G., Chretiennot-Dinet, M. J., Deniaux, B., Devenon, J.-L., Pauc, H.: River discharge and wind influence upon particulate transfer at the land-ocean interaction: Case study of the Rhone River plume, Estuarine Coastal and Shelf Science, 45, 303-316, https://doi.org/10.1006/ecss.1996.0190, 1997.

Olita, A., Sorgente, R., Ribotti, A., Fazioli, L., and Perilli, A.: Pelagic primary production in the Algero-Provençal Basin by means of multisensor satellite data: focus on interannual variability and its drivers, Ocean Dynamics, 61, 1005-1016, https://doi.org/10.1007/s10236-011-0405-8, 2011.

Palanques, A., Durrieu de Madron, X., Puig, P., Fabres, J., Guillén, J., Calafat, A., ... and Bonnin, J.: Suspended sediment fluxes and transport processes in the Gulf of Lions submarine canyons. The role of storms and dense water cascading, Marine Geology, 234, 43-61, https://doi.org/10.1016/j.margeo.2006.09.002, 2006.

Pastor, L., Cathalot, C., Deflandre, B., Viollier, E., Soetaert, K., Meysman, F. J. R., and Rabouille, C. Modeling biogeochemical processes in sediments from the Rhone River prodelta area (NW Mediterranean Sea), Biogeosciences, 8, 1351–1366, https://doi.org/10.5194/bg-8-1351-2011, 2011.

Petrenko, A.: Variability of circulation features in the Gulf of Lion NW Mediterranean Sea. Importance of inertial currents, Oceanologica Acta, 26, 323-338, https://doi.org/10.1016/S0399-1784(03)00038-0.,2003.

Petrenko, A., Dufau, C., and Estournel, C.: Barotropic eastward currents in the western Gulf of Lion, north-western Mediterranean Sea, during stratified conditions, Journal of Marine Systems, 74, 406–428. https://doi.org/10.1016/j.jmarsys.2008.03.004, 2008.

Petrenko A., Leredde, Y., and Marsaleix, P.: Circulation in a stratified and wind-forced Gulf of Lions, NW Mediterranean Sea: In situ and modeling data, Cont. Shelf Res., 25, 1, 7-27, https://doi.org/10.1016/j.csr.2004.09.004, 2005.

Puig, P., Palanques, A., Orange, D. L., Lastras, G., and Canals, M.: Dense shelf water cascades and sedimentary furrow formation in the Cap de Creus Canyon, northwestern Mediterranean Sea, Cont. Shelf Res., 28, 2017-2030, https://doi.org/10.1016/j.csr.2008.05.002, 2008.

Reffray, G., Fraunié, P., and Marsaleix, P.: Secondary flows induced by wind forcing in the Rhône region of freshwater influence, Ocean Dynamics, 54, 179-196, http://10.1007/s10236-003-0079-y, 2004.

Ribera d'Alcalà, M., Civitarese, G., Conversano, F., and Lavezza, R.: Nutrient ratios and fluxes hint at overlooked processes in the Mediterranean Sea, Journal of Geophysical Research: Oceans, 108, https://doi.org/10.1029/2002JC001650, 2003.

Sackmann, B. S., Perry, M. J., and Eriksen, C. C.: Seaglider observations of variability in daytime fluorescence quenching of chlorophyll-a in Northeastern Pacific coastal waters, Biogeosciences Discussions, 5, 2839-2865, https://doi.org/10.5194/bgd-5-2839-2008, 2008.

Sadaoui, M., Ludwig, W., Bourrin, F., and Raimbault, P.: Controls, budgets and variability of riverine sediment fluxes to the Gulf of Lions (NW Mediterranean Sea), Journal of Hydrology, 540, 1002-1015, https://doi.org/10.1016/j.jhydrol.2016.07.012, 2016.

Sanchez-Vidal, A., Higueras, M., Martí, E., Liquete, C., Calafat, A., Kerhervé, P., and Canals, M.: Riverine transport of terrestrial organic matter to the North Catalan margin, NW Mediterranean Sea, Progress in oceanography, 118, 71-80, https://doi.org/10.1016/j.pocean.2013.07.020, 2013.

Sanchez-Vidal, A., Pasqual, C., Kerhervé, P., Calafat, A., Heussner, S., Palanques, A., and Puig, P.: Impact of dense shelf water cascading on the transfer of organic matter to the deep western Mediterranean basin, Geophysical Research Letters, 35, https://doi.org/10.1029/2007GL032825, 2008.

825 Sempéré, R., Charrière, B., Van Wambeke, F., and Cauwet, G.: Carbon inputs of the Rhône River to the Mediterranean Sea: Biogeochemical Implications, Global Biogeochemical Cycles, 14, 669–681, https://doi.org/10.1029/1999GB900069, 2000.

Soetaert, K., Herman, P. M. J., Middelburg, J. J., Heip, C., Smith, C. L., Tett, P., and Wild-Allen, K.: Numerical modelling of the shelf break ecosystem: Reproducing benthic and pelagic measurements, Deep Sea Research II, 48, 3141–3177, https://doi.org/10.1016/S0967-0645(01)00035-2, 2001.

830 Teruzzi, A., Bolzon, G., Salon, S., Lazzari, P., Solidoro, C., and Cossarini, G.: Assimilation of coastal and open sea biogeochemical data to improve phytoplankton simulation in the Mediterranean Sea, Ocean Modelling, 132, 46-60, https://doi.org/10.1016/j.ocemod.2018.09.007, 2018.

Testor P., Mortier, L., Coppola, L., Claustre, H., D'Ortenzio, F., Bourrin, F., Durrieu de Madron, X., and Raimbault, P.: Tucpa deployment (EGO glider: tenuse) (Mediterranean Sea - Western basin), SEANOE, https://doi.org/10.17882/56441, 2018.

835 Thomalla, S. J., Moutier, W., Ryan-Keogh, T. J., Gregor, L., and Schütt, J.: An optimized method for correcting fluorescence quenching using optical backscattering on autonomous platforms, Limnology and Oceanography: Methods, 16, 132-144, https://doi.org/10.1002/lom3.10234, 2018.

Thunell, R., Benitez-Nelson, C., Varela, R., Astor, Y., and Muller-Karger, F. Particulate organic carbon fluxes along upwelling-dominated continental margins: Rates and mechanisms, Global Biogeochemical Cycles, 21,
840 https://doi.org/10.1029/2006GB002793, 2007.

Tusseau-Vuillemin, M. H., Mortier, L., and Herbaut, C.: Modeling nitrate fluxes in an open coastal environment (Gulf of Lions): Transport versus biogeochemical processes, Journal of Geophysical Research: Oceans, 103, 7693-7708, https://doi.org/10.1029/97JC03709, 1998.

Ulses, C., Auger, P.-A., Soetaert, K., Marsaleix, P., Diaz, F., Coppola, L., and Estournel, C.: Budget of organic carbon in the
845 North-Western Mediterranean Open Sea over the period 2004–2008 using 3-D coupled physical-biogeochemical modeling, Journal of Geophysical Research: Oceans, 121, 7026–7055, https://doi.org/10.1002/2016JC011818, 2016.

Ulses, C., Estournel, C., Bonnin, J., Durrieu de Madron, X., and Marsaleix, P.: Impact of storms and dense water cascading on shelf-slope exchanges in the Gulf of Lion (NW Mediterranean). Journal of Geophysical Research 113, C02010, doi:10.1029/2006JC00379, 2008a.

850 Ulses, C., Estournel, C., Durrieu de Madron, X., and Palanques, A.: Suspended sediment transport in the Gulf of Lions (NW Mediterranean): Impact of extreme storms and floods, Cont. Shelf Res., 28, 2048-2070, https://doi.org/10.1016/j.csr.2008.01.015, 2008b.

https://doi.org/10.5194/bg-2021-82
Preprint. Discussion started: 6 April 2021

Ulses, C., Estournel, C., Puig, P., Durrieu de Madron, X., and Marsaleix, P.: Dense shelf water cascading in the northwestern Mediterranean during the cold winter 2005: Quantification of the export through the Gulf of Lion and the Catalan margin, Geophysical Research Letters, 35, https://doi.org/10.1029/2008GL033257, 2008c.